Ecological Monographs, 74(3), 2004, pp. 415–442
© 2004 by the Ecological Society of America

FECUNDITY OF TREES AND THE COLONIZATION–COMPETITION HYPOTHESIS

JAMES S. CLARK,[1,2,3] SHANNON LADEAU,[2] AND INES IBANEZ[2]

[1]*Department of Biology and Nicholas School of the Environment, Duke University, Durham, North Carolina 27708 USA*
[2]*University Program in Ecology, Duke University, Durham, North Carolina 27708 USA*

Abstract. Colonization–competition trade-offs represent a stabilizing mechanism that is thought to maintain diversity of forest trees. If so, then early-successional species should benefit from high capacity to colonize new sites, and late-successional species should be good competitors. Tests of this hypothesis in forests have been precluded by an inability to estimate the many factors that contribute to seed production and dispersal, particularly the many types of stochasticity that contribute to fecundity data. We develop a hierarchical Bayes modeling structure, and we use it to estimate fecundity schedules from the two types of data that ecologists typically collect, including seed-trap counts and observations of tree status. The posterior density is obtained using Markov-chain Monte Carlo techniques. The flexible structure yields estimates of size and covariate effects on seed production, variability associated with population heterogeneity, and interannual stochasticity (variability and serial autocorrelation), sex ratio, and dispersal. It admits the errors in data associated with the ability to accurately recognize tree status and process misspecification. We estimate year-by-year seed-production rates for all individuals in each of nine sample stands from two regions and up to 11 years. A rich characterization of differences among species and relationships among individuals allows evaluation of a number of hypotheses related to masting, effective population sizes, and location and covariate effects. It demonstrates large bias in previous methods. We focus on implications for colonization–competition and a related hypothesis, the successional niche—trade-offs in the capacity to exploit high resource availability in early successional environments vs. the capacity to survive low-resource conditions late in succession.

Contrary to predictions of trade-off hypotheses, we find no relationship between successional status and fecundity, dispersal, or expected arrivals at distant sites. Results suggest a mechanism for maintenance of diversity that may be more general than colonization–competition and successional niches. High variability and strong individual effects (variability within populations) generate massive stochasticity in recruitment that, when combined with "storage," may provide a stabilizing mechanism. The storage effect stabilizes diversity when species differences ensure that responses to stochasticity are not highly correlated among species. Process variability and individual effects mean that many species have the advantage at different times and places even in the absence of "deterministic" trade-offs. Not only does colonization vary among species, but also individual behavior is highly stochastic and weakly correlated among members of the same population. Although these factors are the dominant sources of variability in data sets (substantially larger than the deterministic relationships typically examined), they have not been not included in the models that ecologists have used to evaluate mechanisms of species coexistence (e.g., even individual-based models lack random individual effects). Recognition of the mechanisms of coexistence requires not only heuristic models that capture the principal sources of stochasticity, but also data-modeling techniques that allow for their estimation.

Key words: coexistence; colonization–competition hypothesis; hierarchical Bayes; Markov-chain Monte Carlo; masting; population size, effective; random effects; stochasticity; successional niche; tree fecundity schedule; tree seed production.

INTRODUCTION

Colonization–competition trade-offs may be a stabilizing force for tree diversity (Tilman 1994, Rees et al. 2001). This mechanism requires a trade-off between colonizing and competitive abilities and, thus, a hierarchy of species arranged along these two axes (Tilman 1994). Species that tend to colonize first have high fecundity and broad dispersal. This capacity to colonize early is offset by inferior competitive ability (Horn and MacArthur 1972, Armstrong 1976, Hastings 1980, Caswell and Cohen 1991). The trade-off enhances coexistence by allowing for different species to be favored at different times following disturbance, and the land-

Manuscript received 4 November 2002; revised 21 July 2003; accepted 28 July 2003; final version received 24 September 2003. Corresponding Editor: J. Ver Hoef.
[3] E-mail: jimclark@duke.edu

scape provides continual turnover in terms of newly disturbed sites. By itself, the mechanism has strict requirements in terms of parameters describing colonizing ability and rates of competitive demise. Moreover, there is a limit to how similar the species can be in terms of these parameter trade-offs (Tilman 1994, Holmes and Wilson 1998, Adler and Mosquera 2000). This stringent requirement can be alleviated to some degree by the presence of a second mechanism, the *successional niche*, whereby species trade off competitive ability when resources are scarce (e.g., low light levels long after disturbance) with the capacity to exploit abundant resources that may be present immediately following disturbance (Pacala and Rees 1998). Although both competition–colonization and successional niches require trade-offs, these mechanisms can operate simultaneously (Bolker and Pacala 1999, Rees et al. 2001, Hixon et al. 2002), resulting in the possibility of trade-off combinations that involve both mechanisms. Tree species may possess a suite of traits related to successional status (Oosting 1942, Connell and Slatyer 1977, Christensen and Peet 1984, Huston and Smith 1987, Pacala et al. 1996).

There are no direct tests of the colonization–competition hypothesis in forests, where manipulative experiments are necessarily shorter than tree generations. Experimental tests have been suggested for short-lived plants (Tilman 1994, Pacala and Rees 1998, Bolker and Pacala 1999). Levine and Rees (2002) used seed size as a basis for examining the relationship in annual plants, but perennial plants entail broader challenges. In lieu of long-term field experiments, tests would require two elements. First, colonization capacity needs estimation. If colonization–competition trade-offs maintain diversity, then fecundity and dispersal capacities of early-successional species combine to result in higher probabilities of arriving at new sites than late-successional species. Second, models incorporating those estimates can be used to evaluate whether or not trade-offs with competitive ability could promote coexistence. We address the first component here, by providing estimates of fecundity schedules and dispersal. The second component is the subject of another study (J. S. Clark, M. Dietze, S. Govindarajan, and P. Agarwal, *unpublished manuscript*).

Although there have been numerous efforts to quantify fecundity of trees growing in closed stands, none have produced accurate estimates. Fecundity schedules comprise a complex set of patterns that involve tree size (e.g., Harper 1977, Thomas 1996), location (Greenberg and Parresol 2002) and resource effects (LaDeau and Clark 2001), autocorrelation (dependence in time), synchronicity among individuals that may involve climate and pollen limitation (Koenig and Knops 2000), and sex ratios. Lack of fecundity estimates results from an inability to directly observe seed production. Open-grown trees sometimes provide a basis for whole-tree seed-production estimates (e.g., Koenig et al. 1994). More typically, forests have closed canopies, where seeds can often be seen on trees, but not counted. Observations from towers above the canopy (LaDeau and Clark 2001) are an exception. Where trees are isolated from conspecifics and dispersal distances are low (seed shadows do not overlap), direct calculations based on seed-trap densities provide rough estimates (Downs and McQuilken 1944, Greenberg and Parresol 2002). Seed orchards are of little relevance, because artificially high fecundity of open-grown trees does not apply to closed stands—they are open-grown for a reason. Likewise, onset of reproduction observed for open-grown trees occurs earlier than it does in the understory. We are unaware of sex-ratio estimates for any overstory tree species—a tree with no apparent seed might be male, immature, observed at the wrong time, or seeds may simply be obscured from view. Using inverse methods (Ribbens et al. 1994, Clark et al. 1998, 1999*b*) it has been possible to identify a single fecundity parameter, which is not sufficient to describe the many elements of fecundity schedules. We show here that the many sources of stochasticity that are left out of previous inverse models result in misleading estimates.

We introduce methods to simultaneously estimate a comprehensive range of factors that determine tree fecundity schedules. Developments in computational statistics during the 1990s (Gelfand and Smith 1990, Gelman et al. 1995, Carlin and Louis 2000) allow us to define a high-dimensional model for these joint effects and to estimate the full complement of latent (unobserved) variables and parameters that describe fecundity schedules. Our analysis involves a process model for the fecundity schedule that accommodates the time-series character of seed production in individuals. Because fecundity is a latent process (we cannot directly observe it), we embed this process model within a rich structure that links the latent fecundity process to the two types of data ecologists typically obtain, seed collections and observations of whether or not individual trees are reproductive. The latent fecundity process is estimated tree-by-tree together with "population-level" variables, such as sex ratios, covariate and size effects, and serial (year-to-year) autocorrelation, together with dispersal and the parameters that describe onset of first reproduction. The individual time series, together with their uncertainties, are then available for more extensive investigations of spatial and temporal effects. An unusually large data set involving nine stands from two regions spanning up to 11 years reveals location effects. As part of this analysis we demonstrate how to address the broad challenge of assimilating different types of evidence as the basis for inference at the individual and population levels. Results allow us to evaluate the extent to which species differ at the population and individual levels and to evaluate the extent to which actual fecundity schedules support assumptions of the colonization–competition hypothesis.

Because it will be familiar to ecologists and serve as a point of departure, we begin with a summary of the classical modeling approach. This brief overview provides context and illustrates why previous methods are inadequate. We then describe statistical computation methods that allow us to accommodate full fecundity schedules. Our analysis involves partitioning the deterministic and stochastic factors that contribute to fecundity schedules for all of the dominant canopy species in our two study regions.

STRATEGY

The limitations of traditional methods

Fecundity models are typically allometric (Harper 1977, Thomas 1996). For trees, diameter is the common size variable, because it is readily observed:

$$y_i = \mu_i + \varepsilon_i \tag{1}$$

where y_i is the annual log seed production by the ith tree having log diameter d_i, and

$$\mu_i = \alpha_0 + \alpha_1 d_i \tag{2}$$

is the fecundity process model, where α_0 and α_1 are regression parameters, and ε_i is a zero-mean error process, $\varepsilon_i \sim \mathcal{N}(0, \sigma^2)$. If fecundity is simply proportional to basal area (diameter squared) (e.g., Ribbens et al. 1994, Clark et al. 1998, 1999*b*, Greenberg and Parresol 2002), then $\alpha_1 = 2$ (Fig. 1). If the rate of fecundity increase eventually declines with diameter, as expected when trees become large (Downs and McQuilkin 1944, Greenberg and Parresol 2002), then $0 < \alpha_1 < 1$. The last term in Eq. 1 allows for observation error and process variability on annual seed counts. Observation errors result because counts are imprecise. Process variability is model misspecification. Eq. 1 is not the exact relationship between tree diameter and fecundity, but, rather, an approximation. It is an approximation, because many factors that affect fecundity are not contained in the model. Because fecundity y_i typically cannot be directly observed, this traditional approach is not tenable.

Inverse approaches allow some progress by introducing a transport model for dispersal that translates a process that is obscure (seeds in trees y_i) to data that can be collected (seeds counted in traps s_j)(Ribbens et al. 1994, Clark et al. 1998, 1999*b*). Such models can be written in general terms as

$$s_j \sim \text{Pois}[ATg_j(\mathbf{y})] \tag{3}$$

where A is the area of a seed trap, T is the duration of the study, and $g_j(\mathbf{y})$ is expected seed flux to the ground at location j (seeds per area per year). The Poisson sampling distribution is the sole source of variability, as $g_j(\mathbf{y})$ is a function of a deterministic fecundity process (Eq. 2) and a "mean" dispersal process. This approach entails shortcomings that are unappreciated. A short catalog of problems includes the following:

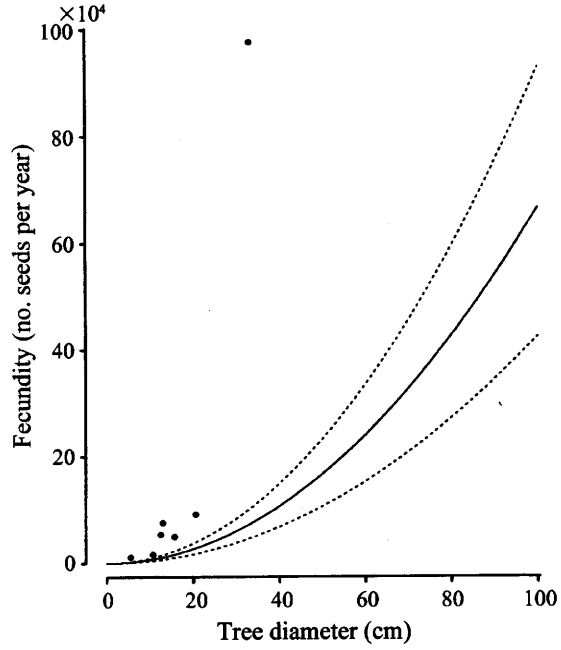

FIG. 1. Seed counts on seven *Acer rubrum* trees from central Massachusetts felled in 1971 (solid circles; Abbott 1974). Also shown is the maximum-likelihood estimate (solid line) with 95% CI (dashed lines) for the fecundity schedule obtained using an inverse modeling approach (Clark et al. 1999*b*).

1) *No process variability.*—Because we cannot observe seed production, we must infer it; fecundity is a latent variable to be estimated, not observed. If we allow no stochasticity in the fecundity process, we assume that Eq. 2 describes seed production exactly. We can "propagate" error in the estimates of α_0 and α_1 to y_i, but that confidence envelope is conditioned on the assumption that there is no stochasticity in the fecundity process. To construct a confidence interval on fecundity that accommodates variability, it must be included in the model.

Inverse methods based on classical statistics (Ribbens et al. 1994, Clark et al. 1999*b*) do not allow for variability in fecundity (*process variability*). The Poisson sampling distribution is not related to fecundity. It does not enter the model at the same place as fecundity, and it has a different structure. Because the seed-trap sampling distribution is the only place that recognizes stochasticity, variability in fecundity will be assumed (in the model) to arise after dispersal. By contrast, Eq. 1 describes process variability that is lognormal—low (but positive) values most years, with occasional high production. If we propagate that variability to seed-trap counts, we could imagine a sampling distribution more dispersed than Poisson (i.e., conditionally Poisson, albeit marginally overdispersed). However, a more dispersed sampling distribution for seed traps (e.g.,

Clark et al. [1998] used a negative binomial) does not permit identification of additional parameters. The shape parameter for the sampling distribution simply trades off with other parameters (Clark et al. 1999*b*). The fact that we cannot include process variability ε_i suggests that parameter estimates could be biased. We will show here that the bias is large.

2) *Time-series considerations.*—Because seed production may be correlated over time, the independent errors (white-noise) assumption of Eq. 1 is unrealistic. Thus, even if we could include process variability in fecundity, we still require a structure that accommodates the autoregressive nature of seed production. In other words, Eq. 1 needs a time component, $y_{it} = \mu_{it} + \varepsilon_{it}$, where the stochastic term allows autocorrelation.

3) *Individual effects.*—The masting phenomenon concerns both individual differences and time. Eqs. 1 and 2 assume that the same fecundity relationship applies to all individuals of a given diameter. We cannot infer variability among individuals if we assume that they are identical. A random component for "individual effects," β_i, might now look like this: $y_{it} = \mu_{it} + \beta_i + \varepsilon_{it}$. This is termed a "mixed model."

4) *Inflexible process model.*—The allometric model does not allow for the fact that trees produce no seeds until maturity, that production can then increase rapidly (LaDeau and Clark 2001), and that it subsequently declines with age (Downs and McQuilkin 1944). In principle, we can add more parameters. In practice, even large data sets from stands containing large trees do not permit identification of additional parameters. Neither Ribbens et al. (1994) nor Clark et al. (1998, 1999*b*) resolved both parameters in Eq. 2; in both cases, parameter α_1 was fixed.

5) *Gender.*—Because seeds may not be observed on a tree for many reasons, we cannot use the regression approach to identify the sex ratio of dioecious species.

6) *Inability to assimilate evidence.*—Point 5 is one aspect of a broader limitation: both seed-trap and status observations could contribute insight on tree fecundity. Eq. 1 requires counts of seeds on trees, which cannot be obtained, and it accommodates neither of the variables that can be observed. The inverse approach accommodates only seeds in traps.

A study that reports direct observations of seed production of forest-grown trees (Abbott 1974) demonstrates the challenges. Seven *Acer rubrum* trees were felled, and seeds were removed and weighed. Subsamples were counted. Total fecundity was estimated based on sample masses. These estimates from closed-canopy conditions show a relationship between fecundity and diameter, with the smallest individual supporting ~12 000 seeds and the largest individual (33-cm diameter) having nearly 10^6 (Fig. 1).

Most aspects of fecundity cannot be determined from this destructive harvest. The snapshot view gives no indication of interannual effects. We do not know if the year 1971 is representative, if there is autocorrelation, or if there are higher-order effects (e.g., masting). Of course, all trees were selected for this study because seeds were evident. We do not know size of maturation or sex ratio, because those estimates would require sampling that is blind as to reproductive status. We cannot separate size effects from individual effects—if size effects explain Fig. 1, then we infer a dramatic increase in fecundity at 25-cm diameter. Alternatively, individual differences might explain the scatter in Fig. 1. Because there is a single year of data, we cannot assess correlations among individuals or through time.

The superimposed schedule for *A. rubrum* estimated in the southern Appalachians contrasts the limitations of seed-rain estimates obtained from a classical framework. Due to high interannual variability, Clark et al. (1999*a*) found that nearly five years of data, pooled across years, were needed to estimate a single fecundity parameter. Because more parameters are not identifiable, the fecundity schedule is unrealistic over much of the size range, increasing too slowly for small trees and too fast for large trees (Fig. 1). Thus, we require extensive data to estimate a single parameter, with no prospect for inferring size and covariate effects, autocorrelation, synchronicity, and tree-to-tree correlation.

A hierarchical Bayes structure

Our model relates seed production to the two types of data ecologists typically collect. Seed traps provide information on fecundity, provided we link those data to the individual trees. Status observations constrain estimates based on seed traps, because they provide explicit information on individuals. We employ a hierarchical Bayes structure that allows us to combine these different data types. It consists of (1) process models, (2) data models, and (3) parameter models. The full hierarchical structure can be represented in terms of these three stages:

$$p(\text{parameters} \mid \text{data, priors})$$

$$\propto p(\text{data} \mid \text{process, data parameters}) \quad (3a)$$

$$\times\, p(\text{process} \mid \text{process parameters}) \quad (3b)$$

$$\times\, p(\text{parameters} \mid \text{priors}) \quad (3c)$$

(Gelfand and Smith 1990, Wikle et al. 2003). The left-hand side of Eq. 3 is a joint distribution of "unobservables" (parameters and latent variables), including those related to the process of interest and those that allow for additional sources of stochasticity (uncertainty and variability).

Our model structure is designed to quantify components of fecundity that have long been recognized. This motivation contrasts with one that would test for hypothetical factors and, consequently, focus on model selection to identify the lowest-dimensional model. Our process models for seed production, maturation, and

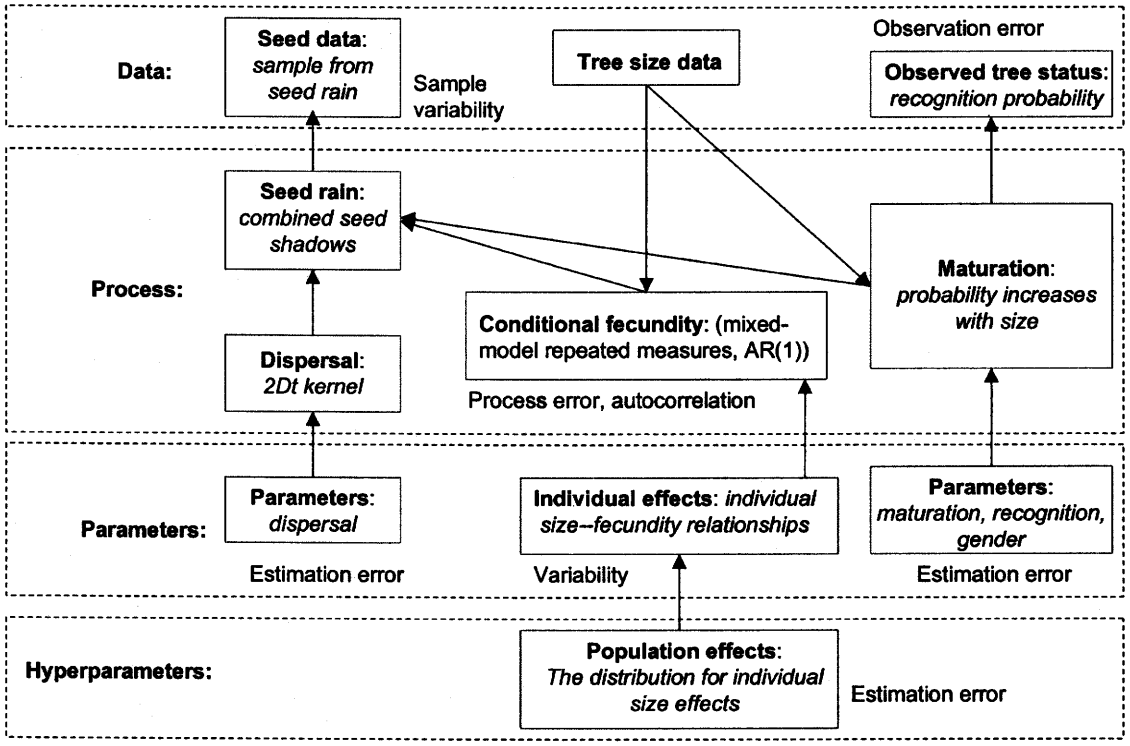

FIG. 2. Model structure for hierarchical Bayes analysis based on Eq. 3. Boxes contain model elements. Sources of stochasticity are in italics.

dispersal (3b) are simple and isolate factors that are well-known. They describe conditional fecundity, reproductive status, and dispersal (Fig. 2: "Process" stage). The conditional fecundity schedule is the seed production of a tree, conditioned on the events that it is mature and (for dioecious species) female.

Because it has long been recognized that masting contributes to fecundity patterns, we estimate the effects of time and individuals. This requires a nonlinear mixed model with longitudinal structure. The model is "mixed" because there is a population-level relationship between diameter and seed production (fixed effects) and additional variability among individuals (random effects). Thus, we allow heterogeneity in the diameter–fecundity relationship and interannual variability, including autocorrelation. The longitudinal structure allows that each tree's schedule is a time series representing a single observation. We develop the simplest possible model that includes these effects.

Due to the nature of observations, there are two additional process models that link seed production of trees to observations of tree status (maturation schedule) and seed counts in traps (dispersal). The maturation schedule describes the increasing probability of maturation with diameter and the sex ratio. The dispersal process distributes tree production to seed traps; it is spatial and based on maps of trees and seed traps. Again, we incorporate the simplest possible process models that are consistent with observations, a sigmoid increase in maturation status (e.g., LaDeau and Clark 2001), one parameter for gender, and one parameter for the dispersal model (Clark et al. 1999*b*).

Data models (Eq. 3a) relate the processes of conditional fecundity, maturation, and dispersal to observations (Fig. 2: "Data" stage). The data model for tree status assigns probabilities to each type of observation (seeds not observed, seeds present, male flowers present and no seeds) conditioned on the true state of the tree (immature, female and mature, male and mature). This is a model for recognition error. The data model for seed rain relates the seed density predicted for a spatial location to seed counts based on the collecting area of traps and sampling stochasticity. Again, we emphasize simplicity, with one parameter for recognition probability. No new parameters are required for the Poisson sampling distribution of seed traps. Parameter models (Eq. 3c) allow for stochasticity and consist of priors and hyperpriors (Fig. 2: "Parameter" stage). Individual effects represent an additional stage ("Hyperparameter" stage), which we might choose to label as a level "3d."

Model complexity

There are two reasons why we do not pursue model selection. First, despite the high dimensionality de-

manded by our approach, ours is, in fact, a "minimal model," including only basic features of fecundity schedules and processes that link those schedules to different data types. Complexity in our model comes from a large number of latent variables represented by seed production by every tree, in every year. We are not "testing" for individual or temporal effects; the effects are well known and the basis for a large literature on masting. Their quantification is critical for understanding how fecundity varies among individuals and over time. Estimation has been the challenge, and it is our focus. Despite the unavoidable complexity represented by estimating seed production by every tree every year, our parsimonious modeling strategy involves only 10 population-level parameters per species. We will see that, for many species, temporal effects overwhelm all other factors. For these species, model selection would say that we can ignore all other effects (including tree size). Our goal is to "see through" the large variability contributed by such effects and determine their relative importances. In a similar vein, Lange et al. (1992) analyze responses of HIV progress to treatment, the clinicial question, despite the fact that simpler models would "explain" the data.

Second, there is no consensus on model-selection methods for hierarchical models (Gelfand and Dey 1994). Many have been proposed, and all generate some debate (e.g., Spiegelhalter et al. 2002). Again, because we are not attempting to "test" for size, year, or individual effects, but rather to quantify their contributions, we focus on parameterization of this minimal model.

Methods

Process and parameter models

To exploit both types of data, we express fecundity in terms of a maturation schedule θ, i.e., the probability of being in the reproductive state, and conditional fecundity, i.e., the production of seed given that an individual is reproductive. Fecundity is the product of these two quantities, $F = \theta 10^y$.

To account for the range of stochastic sources expected to influence fecundity, we develop a mixed model with fixed and random effects for repeated measures with autocorrelated error. Let T_i be the number of years in the fecundity series for tree i. The likelihood for the ith tree is a multivariate normal of dimension T_i:

$$\mathcal{N}_{T_i}(\mathbf{y}_i | \mathbf{X}_i\boldsymbol{\alpha} + \mathbf{1}\beta_i, \boldsymbol{\Sigma}_i). \tag{4}$$

Here, $\mathbf{y}_i$ is the $T_i \times 1$ vector of annual seed production for the ith tree, to distinguish it from the seed production of the ith tree in year t, designated as y_{it}. $\mathbf{X}_i$ is the $T_i \times 2$ design matrix:

$$\mathbf{X}_i = \begin{bmatrix} 1 & d_{it} \\ \vdots & \vdots \\ 1 & d_{iT_i} \end{bmatrix} \tag{5}$$

where d_{it} is log diameter for the ith tree in year t, $\boldsymbol{\alpha} = [\alpha_0, \alpha_1]^T$ is the vector of parameters for "fixed effects," $\mathbf{1}$ is the $T_i \times 1$ vector of ones, β_i are individual random effects, and $\boldsymbol{\Sigma}_i$ is the covariance matrix for seed production across years.

Population heterogeneity enters as random effects (Laird and Ware 1982, Lange et al. 1992). The parameter vector $\boldsymbol{\alpha}$ applies to the whole population and operates on the "fixed effects" in $\mathbf{X}_i$. The random effect of individual i is described by β_i. Thus, we assume that the size effects are consistent in shape (parameter α_1), but can vary individually in strength (parameter β_i). Because each individual is represented by a small range of diameter change, we did not include individual effects on shape parameter α_1.

We additionally provide for autocorrelation (e.g., Lindsey 1999:106). For individual i, the covariance matrix with autoregressive (AR(1)) structure is

$$\boldsymbol{\Sigma}_i = \frac{\sigma^2}{1-\rho^2}\begin{bmatrix} 1 & \rho & \rho^2 & \cdots & \rho^{T_i-1} \\ \rho & 1 & \rho & & \\ \rho^2 & \rho & 1 & & \\ \vdots & & & \ddots & \rho \\ \rho^{T_i-1} & & & \rho & 1 \end{bmatrix} \tag{6}$$

with total variance σ^2, and autocorrelation ρ. Note that the covariance matrix depends on individual i only in dimension (two individuals with the same sampling duration T_i have the same covariance matrix). In our implementation, estimates of σ^2 and ρ apply to the full population. Together, the random effects and autoregression capture variability and fulfill assumptions that fecundities are conditionally independent (they are marginally dependent). The general structure for this portion of the model follows Laird and Ware (1982; see Lange et al. [1992] for a Markov-chain Monte Carlo (MCMC) implementation).

Parameter models fill out the fecundity submodel. The random effects β_i are normally distributed with mean zero and variance τ^2, $p(\beta_1, \ldots, \beta_m | \tau^2) = \prod_{i=1}^m \mathcal{N}(\beta_i | 0, \tau^2)$, the prior for which is inverse gamma $\mathrm{IG}(\tau^2 | a_\tau, b_\tau)$ and defines the third stage that makes the fecundity submodel hierarchical. Parameters for fixed effects have prior $\mathcal{N}_2(\boldsymbol{\alpha} | \mathbf{c}, \mathbf{V}_a)$, with mean vector $\mathbf{c}$ and parameter covariance matrix $\mathbf{V}_a$. The total variance σ^2 on conditional fecundity has an inverse gamma (*IG*) prior (Appendix).

The second process model describes maturation. Let Q_i be the status of tree i, assuming values of zero (not yet reproductive) or one (mature). The probability of maturity,

$$p(Q_i) = \mathrm{Bernoulli}(Q_i | \theta_{it}) \tag{7}$$

increases with tree diameter. A gamma cumulative-distribution (CGam) function describes this schedule:

$$\theta_{it} = \mathrm{CGam}(10^{d_{it}}; a_\theta, b_\theta). \tag{8}$$

The fraction of females for dioecious species is described by parameter ϕ. Tree status Q_i does not have

a time subscript, because observations were not taken each year, and a single status value was assigned to each tree. This assumption should not be applied for long time series, where many trees would change status during the course of the study.

The third process model is dispersal. The expected number of seeds to arrive at location j is determined by the seeds contributed by each tree. We use a two-dimensional Student's t density (2Dt),

$$f(r_{ij}) = \frac{1}{\pi u\left(1 + \frac{r_{ij}^2}{u}\right)^2} \tag{9}$$

for distance r_{ij} (m) between seed trap j and tree i and dispersal parameter u (m^2), because it describes well the pattern of dispersal for a large number of species (Clark et al. 1999*b*). Rotational symmetry means that direction is suppressed, and the density has units of m^{-2}. The fraction of seed that is deposited in a trap of area A is approximately $\int_A f(r)\, dr \approx f(r)A$. The "degrees-of-freedom" parameter determines rare long-distance dispersal, and is not well identified by data. We use a value of 3, which describes dispersal well for distances up to 100 m.

Data models

The two data models involve different observation errors. Data models translate the underlying processes to the data that are observed.

Tree status.—Tree status is observed with error; if seeds are observed, then maturity is certain. But seeds may be missed, because they are obscure in the canopy, seed production can be low, or the timing of observations may not coincide with visible seeds on trees. Begin with a monecious species; the population consists of mature and immature individuals. Let q_i represent the event that an individual is identified as reproductive ($q_i = 1$) or not ($q_i = 0$), Q_i be the corresponding status of the tree (mature and immature, respectively), and let v be the probability that a mature individual will be recognized as such. The probabilities associated with status are $p(Q_i = 1) = \theta$ and $p(Q_i = 0) = 1 - \theta$ (Eq. 8). Then $p(q_i | Q_i = 1) = \text{Bernoulli}(q_i | v)$. We assume that $p(q_i = 1 | Q_i = 0) = 0$, and $p(q_i = 0 | Q_i = 0) = 1$ (observers do not invent seeds). Thus, we are concerned with the probabilities for correct identifications $p(q_i = 1 | Q_i = 1) = v$ and "mistakes" $p(q_i = 0 | Q_i = 1) = 1 - v$. With these assumptions we have the following probabilities for observations:

$$p(q_i = 1) = p(q_i = 1 | Q_i = 1) \times p(Q_i = 1) = v\theta_i \tag{10a}$$

$$\begin{aligned} p(q_i = 0) &= p(q_i = 0 | Q_i = 0)p(Q_i = 0) + p(q_i = 0 | Q_i = 1)p(Q_i = 1) \\ &= 1 \times (1 - \theta_i) + (1 - v)\theta_i = 1 - v\theta_i. \end{aligned} \tag{10b}$$

For a monecious species, the likelihood for the entire data set is the following:

$$\begin{aligned} p(\mathbf{q}) &= \prod_{i,q_i=1} v\theta_i \prod_{i,q_i=0} (1 - v\theta_i) \\ &= \prod_{i=1}^{m} \text{Bernoulli}(q_i | v\theta_i). \end{aligned} \tag{11a}$$

Dioecious plants can be recognized as male and reproductive ($q = 2$), female and reproductive ($q_i = 1$), or unknown ($q_i = 0$). The fraction of females is ϕ, and the sex ratio (females:males) is $\phi/(1 - \phi)$. The likelihood is taken over the three classes:

$$\begin{aligned} p(\mathbf{q}) &= \prod_{i,q_i=1} v\phi\theta_i \prod_{i,q_i=2} v(1 - \phi)\theta_i \prod_{i,q_i=0} (1 - v\theta_i) \\ &= \prod_{i=1}^{m} \text{Multinom}(q_i | 2, \mathbf{w}) \end{aligned} \tag{11b}$$

with the vector of probabilities $\mathbf{w}$ having elements $w_1 = v\phi\theta_i$, $w_2 = v(1 - \phi)\theta_i$, and $w_3 = 1 - w_1 - w_2$. Note that if males cannot be recognized as such, the likelihood collapses to $p(\mathbf{q}) = \Pi_{i,q_i=1} v\phi\theta_i \Pi_{i,q_i=0} 1 - v\phi\theta_i$, and v and ϕ are not independently identifiable. We assume that the same recognition errors apply to males and females.

Seed rain.—The annual seed density observed in seed trap j in year t is conditionally Poisson:

$$s_{jt} \sim \text{Pois}[A_j g_j(\mathbf{y}_t)] \qquad j = 1, 2, \ldots, n \qquad t = 1, \ldots, P_j \tag{12}$$

with expected seed rain $A_j g_j(\mathbf{y}_t)$ determined by the full set of trees that contribute seed to trap j in year t. P_j is the number of years contributing seed to trap j. This expectation is the product of the collection area of the trap, a known constant A_j, and the expected seed arrival per unit area, $g_j(\mathbf{y}_t)$. The expected contribution from tree i to seeds in trap j depends on the probability that it is mature, which increases with diameter, described by θ_{it}, the probability that it is correctly identified as such v, (for dioecious species) the probability that it is female ϕ, and the production of seed conditioned on reproductive status, y_{it}. The fraction of that seed that falls in seed trap j is approximately $f(r_{ij})A_j$, where $f(r_{ij})$ is the density of seed per square meter (Eq. 9). The expected seed per unit area in year t is

$$g_j(\mathbf{y}_t) = \sum_{i=1}^{m} 10^{y_{it}} \delta_{it} f(r_{ij}) \qquad j = 1, \ldots, m \tag{13}$$

and δ_{it} contributes information from tree status observations:

$$\delta_{it} = p(Q_i = 1 | q_i) = \begin{cases} \phi \dfrac{\theta_{it}(1 - v)}{1 - v\phi\theta_{it}} & q_i = 0 \\ 1 & q_i = 1 \\ 1 - v & q_i = 2. \end{cases} \tag{14}$$

In other words, the expected contribution from tree i to the jth trap in year t is is $10^{y_{it}} f(r_{ij})$ if seeds are observed on the tree ($q_i = 1$), and $10^{y_{it}}(1 - v)f(r_{ij})$ if

it is identified as a male ($q_i = 2$), the factor $(1 - v)$ representing the probability that seeds were present despite not having been observed (in which case the tree is actually female). For indeterminant trees ($q_i = 0$), the expectation is the product of $10^{y_{it}} f(r_{ij})$ and the event that it is mature θ_{it}, it is female ϕ, and it was not recognized as seed bearing, despite being so $(1 - v)$ divided by the probability that $q_i = 0$.

The full model

Combining data, process, and parameter models we have the joint posterior:

$$
\begin{aligned}
&p(\boldsymbol{\alpha}, \boldsymbol{\beta}, \sigma^2, \rho, \mathbf{y}, \tau^2, a_\theta, b_\theta \mid \mathbf{X}, \mathbf{s}, \mathbf{q}, \ldots) \\
&\propto \prod_{t=1}^{T_j} \prod_{j=1}^{n} \mathrm{Pois}[s_{jt} \mid A_j g_j(\mathbf{y}_t \mid u, a_\theta, b_\theta, \phi, v)] \\
&\quad \times \prod_{i=1}^{m} \mathrm{Multinom}(q_i \mid 1, w_i) \\
&\quad \times \prod_{i=1}^{m} \mathcal{N}_{T_i}(\mathbf{y}_i \mid \mathbf{X}_i \boldsymbol{\alpha} + 1\beta_i, \boldsymbol{\Sigma}_i) \\
&\quad \times \mathcal{N}_2(\boldsymbol{\alpha} \mid \mathbf{c}, \mathbf{V}_a) \prod_{i=1}^{m} N(\beta_i \mid 0, \tau^2)\mathrm{Gam}(\sigma^2 \mid a_\sigma, b_\sigma) \\
&\quad \times \mathrm{Unif}(\rho \mid -1, 1) \\
&\quad \times \mathrm{Gam}(a_\theta \mid a_0, b_0)\mathrm{Gam}(b_\theta \mid a_0, b_0)\mathrm{Gam}(u \mid a_u, b_u) \\
&\quad \times \mathrm{Unif}(v \mid 0, 1)\mathrm{Unif}(\phi \mid 0, 1) \\
&\quad \times \mathrm{IG}(\tau^2 \mid a_\tau, b_\tau) \qquad (15)
\end{aligned}
$$

where ellipses (" . . . ") represent prior parameter values. Deterministic elements are Eqs. 5, 6, 8, 9, 11, 13, and 14. The monoecious case uses the Bernoulli likelihood Eq. 11a and the dioecious uses Eq. 11b.

This high-dimensional posterior is intractable—we cannot solve it, but we can simulate it using MCMC. The basic structure is a Gibbs sampler (Gelfand and Smith 1990), within which we embed Metropolis and Metropolis-Hastings steps (Hastings 1970). The Gibbs sampler involves alternately sampling from conditional posteriors. Not all conditionals are available, so Metropolis and Metropolis-Hastings steps are used in these cases. The algorithms and prior parameter values are provided in the Appendix. Parameter estimates for species having seeds that could not be confidently differentiated were fitted as combined data sets followed by extraction of species effects based on tree-by-tree estimates of y_{it} and β_i. This was the case for *Acer*, *Carya*, *Magnolia*, *Pinus*, *Quercus*, and *Ulmus*. Although seeds of most of these species can often be identified to the species level, substantial numbers of indistinguishable seeds made our approach preferable. The analysis allows this separation of morphologically similar seeds based on the individual effects assigned to each tree that can be re-aggregated post hoc. It relies on the assumption that most parameters will be similar within a genus, with species effects summarized by the source strength parameter α_0 and heterogeneity summarized by variance τ^2. Thus, estimates can "borrow" information from the combined data from related species for most parameters, while allowing for departures that can be due to species differences or individual effects (see Appendix).

Priors and convergence

Most statisticians would agree that prior parameter values should incorporate existing knowledge. Some ecologists are suspicious of informative priors. For statisticians, we apply realistic prior mean values. However, we neutralize these values by ensuring that the spread of prior densities is sufficiently large as to make them noninformative; they do not have discernable impact on results. We recognize that many statisticians would disagree with this omission of some well-established information on fecundity.

Our "most informative" priors enter the regression and maturation aspects of the model. For the regression, prior means are $\mathbf{c} = [2, 0.5]^T$. The prior covariance matrix, $\mathbf{V}_\alpha = \mathrm{Diag}(1000, 1)$ renders the first prior meaningless, but, had our sample sizes been small, would have provided some weight to the second. The value $c_2 = 0.5$ reflects the fact that fecundity cannot increase in step with diameter indefinitely. Although given a modest prior variance of 1, this prior mean is swamped by data (this effect is evident even from marginal posteriors given in the Appendix). The gamma parameters for maturation status contain a hint of prior knowledge. For a_θ, $a_0/b_0 = 0.2/0.1$ gives a prior mean of 2. For b_θ, $a_0/b_0 = 0.1/1$ gives a prior mean of 0.1. Together, these prior means imply a "half" maturation at 20 cm. But the low values of prior parameters imply prior variances that are too large to affect estimates.

The prior dispersal parameter has gamma prior values of $a_u/b_u = 1/0.01$ implying a prior mean of 100 m^2, but, again, has a variance too large to affect estimates. Variance prior parameters for inverse gamma distributions are 0.01. The uniform priors on the full range of possible values for ρ, v, and ϕ are noninformative.

Convergence can be difficult to assess for high-dimensional models (e.g., Carlin and Louis 2000). Despite the high dimensionality of our model, the MCMC is quite stable. Stability of the algorithm derives from the fact that combinations of seed traps constrain estimates for nearby trees. There are limited combinations of seed-trap estimates that could "satisfy" seed-rain data, with seed traps most influenced by nearby trees. Tree-status estimates add further constraints. To build confidence in convergence, we initialized multiple chains from dispersed values. Each "chain" represents a simulation. Slowest to converge are the latent variables represented by individual seed-production rates for stands having high stem density for a species. It is not possible to monitor every latent parameter.

TABLE 1. Stands sampled for fecundity estimates in two regions in North Carolina, USA.

Stand	Setting, vegetation	Elevation (m)	Map area (ha)	No. seed traps, n	No. years, T
Southern Appalachians					
C1	ridgetop oak–pitch pine	775	0.64	20	11
C2	cove hardwood	830	0.64	20	11
C3	mixed oak	870	0.64	20	11
C4	mixed oak	1100	0.64	20	11
C5	northern hardwoods	1380	0.64	20	11
CL	cove hardwood	1005	2.3	70	2
CU	mixed oak	1010	1.5	43	2
Piedmont					
DB	pine–oak–bottomland hardwood	140	4.1	128	3
DH	pine–oak	135	1.0	30	4

However, we monitored chains for individuals selected at random, and we calculated Gelman and Rubin's (1992) scale-reduction factor. For typical stem densities, convergence was satisfactory by 1000 iterations. We discarded a burn-in (preconvergence values; Gelman et al. 1995) of >2000 iterations for most species and up to 15 000 iterations for species that occurred at especially high densities.

Predictions and forecasts

The approach is used to predict fecundity for as-yet-unobserved trees, stands, and years and to forecast ahead seed production. Let $y_{it}^{(g)}$ be the estimate of log conditional fecundity for the ith individual in year t at the gth step of the MCMC chain, and $\theta_{it}^{(g)}$ be the maturation probability for an individual of log diameter d_{it} calculated from the gth estimates of a_θ and b_θ. Then the posterior distribution of fecundity estimates is assembled from

$$F_{it}^{(g)} = \theta_{it}^{(g)} \times 10^{y_{it}^{(g)}}. \tag{16}$$

To predict fecundities we incorporate posterior information on parameter uncertainty and process variability. If the tree in question is one for which data have been collected up through year t, we have the one-step-ahead fecundity forecast,

$$\hat{F}_{i,t+1} = \theta_{it} \times 10^{\hat{a}_0+\hat{\beta}_i+\varepsilon_{i,t+1}} d_{it}^{\hat{a}_1} \tag{17}$$

with the lag-1 autoregressive [AR(1)] process,

$$\varepsilon_{i,t+1} \sim \mathcal{N}(\hat{\rho}\varepsilon_{i,t}, \hat{\sigma}^2). \tag{18}$$

The individual effect is contained in the deterministic part of the model, because we have estimated it for the individual at hand. Our predictive distribution is obtained by marginalizing over the posterior for fecundity parameters and over the stochastic term, which includes process variability and serial correlation. This process integrates the stochasticity contributed by parameter uncertainty and by variability.

For an individual and year selected at random, individual effects become part of the stochastic term (we do not have an individual estimate β_i). Moreover, lack of previous fecundity estimates means that we cannot use the estimate of autocorrelation to constrain the forecast; thus,

$$\hat{F}_i = \hat{\theta}_i \times 10^{\hat{a}_0+\beta_i+\varepsilon_i} d_i^{\hat{a}_1} \tag{19}$$

where the variability terms are

$$\beta_i + \varepsilon_i \sim \mathcal{N}(0, \hat{\tau}^2 + \hat{\sigma}^2). \tag{20}$$

Note that this zero mean noise term has variance contributed by the process variability and by individual effects.

STUDY REGIONS

Our study involves mapped stands that span a range of environmental settings. Stands are located in two regions, the southern Appalachians and the Piedmont of central North Carolina (Table 1). Sampled stands range in area from 0.64 to 4.1 ha. Southern Appalachian sites include mixed oak (at several elevations), cove hardwoods, mixed hemlock, ridgetop pitch pine, and northern hardwoods. Piedmont sites are mixed pine and hardwood (Table 1).

DATA

Two data types include seed traps and status estimates. Seed traps were deployed in mapped stands. Traps 0.42 × 0.42 m (square) or 0.40-m diameter (round) are supported by pvc pipes at a height of 1.2 m. Traps have wire covers (to minimize rodent losses) and hardware cloth that suspends seeds above trap bases. Holes in trap bases provide drainage. Collection efficiencies of traps are reported in Clark et al. (1998). Collection periods began in 1991 (five Coweeta stands), 1998 (Duke Forest stand DH), 1999 (DB), and 2000 (Coweeta CL and CU) (Table 1). Seeds are recovered from traps 3 to 12 times annually, sorted, identified, counted, and archived at the Duke University Phytotron.

To determine reproductive status, trees were visited during flowering and fruiting seasons and in winter. For many trees, reproductive status is uncertain, because failure to observe seeds does not mean that trees are immature. In our study regions, dioecious species include *Acer rubrum*, *Nyssa sylvatica*, and *Fraxinus amer-*

TABLE 2. Data-set characteristics and posterior mean parameter estimates with 95% confidence credible intervals (upper and lower bounds are listed below mean estimates), by type of tree seed dispersal mechanism.

Tree species	No. plots	No. trees	Total no.		Log likelihood	
			Tree years	Trap years	Seed rain	Tree reproductive status
Taxa with wind-dispersed seed						
Acer spp.	9	4774	22 172	1830	−5430	−12 460
Betula lenta	5	50	536	1020	−8665	−238
Carpinus caroliniana	2	188	658	504	−166	−96
Fraxinus americana	5	808	2954	1084	−1040	−242
Liquidambar styraciflua	2	1303	4118	504	−959	−539
Liriodendron tulipifera	8	862	2982	1610	−5767	−847
Oxydendrum arboreum	7	617	3743	1490	−4870	−1222
Pinus spp.	4	534	1968	944	−1387	−1201
Tsuga canadensis	7	348	1677	1326	−525	−222
Tilia americana	2	76	836	440	−1000	−1
Ulmus spp.	2	1027	3265	504	−947	−360
Taxa with animal-dispersed seed						
Carya spp.	9	1010	4032	1830	−609	−851
Cercis canadensis	2	286	504	875	−195	−352
Cornus florida	8	1588	5927	1610	−360	−1408
Magnolia	6	239	1459	1106	−46	−91
Nyssa sylvatica	8	1305	6190	1610	−1243	−274
Quercus	9	1623	8936	1830	−3629	−2607
Robinia pseudo-acacia	6	102	528	1160	−31	−1
Total		16 740	72 485	21 277		

Note: See Table 3 for taxa fitted to more than one species.

† For population-level parameter estimates, α_0, α_1, and σ^2 are regression parameters; ρ = autocorrelation; τ^2 = variance for individual effects; μ = dispersal parameter; a_0, b_0 = maturation parameters; ϕ = female fraction (dioecious species); and ν = recognition success.

TABLE 2. Extended.

Population-level parameter estimates†									
α_0	α_1	σ^2	ρ	τ^2	μ (m)	a_θ	b_θ	ϕ	ν
2.77	0.406	1.18	0.0361	0.0247	62.0	1.15	0.0508	0.468	0.896
2.75	0.380	1.17	0.0268	0.0167	59.7	1.10	0.0472	0.457	0.892
2.80	0.434	1.20	0.0479	0.0314	64.0	1.19	0.0547	0.481	0.901
4.41	−0.168	2.307	−0.547	0.0630	413.9	4.901	0.2194		0.750
3.86	−0.496	2.023	−0.617	0.0162	396.7	4.784	0.2151		0.735
4.88	0.170	2.608	−0.479	0.1450	430.5	5.026	0.2223		0.769
1.53	0.923	1.360	−0.022	0.0206	50.5	16.110	2.1250		0.532
1.33	0.671	1.186	−0.132	0.0065	39.4	10.410	1.3580		0.462
1.69	1.235	1.604	0.080	0.0402	65.7	21.770	2.8830		0.607
2.28	0.425	1.708	0.105	0.0153	34.7	3.108	0.1444	0.907	0.260
2.19	0.299	1.625	0.061	0.0080	29.9	2.815	0.1236	0.860	0.218
2.34	0.542	1.779	0.140	0.0363	41.2	3.428	0.1733	0.945	0.317
2.31	0.527	0.576	−0.790	0.0018	518.0	5.301	0.1537		0.681
2.28	0.495	0.550	−0.807	0.0010	435.0	5.118	0.1463		0.647
2.34	0.562	0.610	−0.771	0.0029	593.3	5.647	0.1648		0.739
3.37	0.577	0.559	0.371	0.0054	719.8	3.098	1.271		0.453
3.32	0.537	0.531	0.338	0.0037	677.6	3.011	0.1217		0.428
3.42	0.620	0.585	0.399	0.0088	769.6	3.235	0.1335		0.483
2.05	0.681	1.306	0.743	0.0022	40.5	3.255	0.1226		0.559
1.80	0.439	1.256	0.720	0.0007	38.2	3.144	0.1181		0.539
2.30	0.863	1.370	0.762	0.0058	42.8	3.357	0.1286		0.576
2.06	0.700	0.723	−0.349	0.1655	1706.1	1.657	0.0386		0.549
1.78	0.540	0.671	−0.417	0.1391	1439.9	1.517	0.0335		0.519
2.28	0.876	0.787	−0.283	0.1924	2037.8	1.813	0.0435		0.580
1.39	0.669	1.557	−0.421	0.2255	83.3	3.524	0.1616		0.453
1.30	0.559	1.420	−0.469	0.1537	57.0	3.081	0.1272		0.342
1.53	0.772	1.696	−0.361	0.3183	112.8	4.130	0.2111		0.541
1.89	0.470	2.309	0.178	0.0153	7.6	7.105	0.2257		0.006
1.73	0.314	2.057	0.087	0.0013	6.6	6.359	0.1850		0.001
2.08	0.599	2.520	0.263	0.0883	8.8	7.815	0.2667		0.024
2.27	0.888	0.259	0.075	0.2703	306.2	6.250	0.4204		0.466
2.20	0.791	0.197	−0.039	0.2351	238.6	4.719	0.2963		0.415
2.34	0.970	0.313	0.189	0.3154	391.2	8.479	0.6135		0.516
1.02	0.794	0.637	0.266	0.0106	38.1	7.911	0.2843		0.738
0.96	0.732	0.616	0.228	0.0025	31.1	7.364	0.2607		0.692
1.10	0.861	0.656	0.305	0.0234	46.3	8.621	0.3148		0.780
1.62	0.757	0.379	0.272	0.0401	163.9	2.841	0.7680	1.000	0.414
1.51	0.555	0.325	0.165	0.0085	113.5	1.784	0.4122	1.000	0.338
1.71	0.982	0.425	0.380	0.0935	241.6	4.386	1.3550	1.000	0.494
1.21	0.408	0.841	−0.641	0.0124	0.8	4.287	0.8190		0.221
1.17	0.374	0.803	−0.664	0.0079	0.6	3.434	0.6069		0.197
1.23	0.454	0.870	−0.623	0.0213	0.9	5.025	1.0020		0.244
0.58	0.505	0.264	0.095	0.0780	102.2	3.651	0.1656		0.583
0.53	0.430	0.239	0.015	0.0594	69.9	2.977	0.1304		0.500
0.64	0.577	0.283	0.159	0.1015	134.3	4.230	0.2031		0.629
1.60	0.329	1.169	−0.001	0.4349	27.7	3.070	0.0623	0.988	0.351
1.51	0.238	1.115	−0.043	0.3936	25.7	2.945	0.0571	0.960	0.307
1.72	0.430	1.226	0.037	0.5022	29.9	3.205	0.0685	0.998	0.382
1.85	0.571	0.695	0.353	0.0073	37.3	2.701	0.0478		0.575
1.77	0.510	0.669	0.326	0.0035	32.8	2.469	0.0433		0.530
1.92	0.624	0.722	0.383	0.0110	42.4	2.876	0.0517		0.616
0.46	0.546	0.458	0.252	0.0514	17.9	2.743	0.2186		0.003
0.31	0.418	0.398	0.132	0.0027	7.1	0.830	0.1444		0.001
0.61	0.697	0.538	0.386	0.1232	31.6	4.358	0.2949		0.014

TABLE 3. Species-level parameters with 95% credible intervals (upper and lower bounds in parentheses) for taxa fitted at the genus level to more than one species (see Appendix for description of species-level estimates).

Tree species	α_0	τ^2
Acer rubrum	2.77 (2.75–2.80)	0.0246 (0.0158–0.0313)
A. saccharum	2.77 (2.73–2.81)	0.0256 (0.0158–0.0313)
Pinus rigida	1.50 (1.24–1.75)	0.1412 (0.1331–0.2039)
P. taeda	2.10 (1.83–2.39)	0.1457 (0.1331–0.2039)
P. echinata	2.13 (1.85–2.40)	0.1405 (0.1331–0.2039)
Ulmus ind.	2.18 (2.10–2.26)	0.0829 (0.2258–0.3166)
U. alata	2.25 (2.20–2.80)	0.1697 (0.2258–0.3166)
U. rubra	2.89 (2.71–3.72)	0.2258 (0.0667–0.3166)
U. americana	2.24 (2.12–2.37)	0.2258 (0.1029–0.3166)
Carya ind.	1.02 (0.95–1.10)	0.0116 (0.0026–0.0227)
C. tomentosa	1.02 (0.94–1.10)	0.0116 (0.0026–0.0227)
C. glabra	1.02 (0.95–1.10)	0.0116 (0.0026–0.0227)
Magnolia acuminata	0.61 (0.42–0.80)	0.0779 (0.0565–0.1023)
M. Fraseri	0.60 (0.45–0.74)	0.0708 (0.0565–0.1023)
Quercus alba	1.85 (1.77–1.93)	0.0073 (0.0034–0.0112)
Q. coccinea	1.84 (1.76–1.92)	0.0073 (0.0034–0.0112)
Q. falcata	1.85 (1.76–1.94)	0.0074 (0.0034–0.0112)
Q. marylandica	1.84 (1.76–1.93)	0.0074 (0.0034–0.0112)
Q. phellos	1.85 (1.77–1.93)	0.0073 (0.0034–0.0112)
Q. prinus	1.84 (1.76–1.92)	0.0073 (0.0034–0.0112)
Q. rubra	1.85 (1.76–1.92)	0.0073 (0.0034–0.0112)
Q. stellata	1.85 (1.77–1.93)	0.0073 (0.0034–0.0112)
Q. velutina	1.84 (1.76–1.92)	0.0073 (0.0034–0.0112)
Q. ind.	1.84 (1.76–1.93)	0.0073 (0.0034–0.0112)

icana. On each occasion, individual trees were scored as reproductive, not reproductive, or uncertain. Dioecious species were identified as males if they flowered but did not bear fruit, and as females otherwise. For *A. rubrum*, flower morphology was used as an additional check, but could only be used if flowers could be reached. There are uncertainties in all identifications, quantification of which is one goal of this analysis.

RESULTS

We obtained estimates of all parameters and latent variables in Fig. 2 for 20 species. Other species present on our plots for which trees, seeds, or both were too rare to provide estimates included *Acer barbatum* (DB, DH), *Ostrya virginiana* (DB, DH), *Sassafras albidum* (C1), *Betula alleghaniensis* (C5), *Juglans nigra* (DB), *Juniperus virginiana* (DB, DH), *Prunus serotina* (DB, DH), *Morus rubra* (DB, DH), *Fagus grandifolia* (DB, C1, C5) (see Table 1 for stand code).

Observations

This analysis involves unusually large data sets (72 485 tree-years and 21 277 trap-years) and many estimates. There are 200 parameters, 10 for each species that describe "population-level" processes and stochasticity (Tables 2 and 3). There are an additional 16 740 parameters, describing random individual effects (one for every tree in the data set), and 72 485 latent variables (one for every tree, every year). Because space admits only a small subset of our analysis, we provide detail for one species and consider key relationships for others. *Acer rubrum* is the example, because trees and seeds are abundant on all plots, and it is dioecious. Convergence is discussed in the Appendix. Seed rain varied widely among traps and years (Fig. 3). *Acer rubrum* and *A. saccharum* have morphologically similar seeds and were fitted together (Appendix). *Acer* seeds and trees occurred at all nine stands, with a total of 4774 trees, 22 172 tree-years, 371 traps, 1830 trap-years, and 21 383 seeds. Of 4631 *A. rubrum* trees, 575 were identified as male, 439 as female, and 3617 as indeterminate. The remaining 140 *A. saccharum* trees included in this fit were primarily in plot C5, and only two individuals were identified as reproductive. For *A. rubrum*, bright-red flowers and fruits were apparent, so most large trees could be recognized as reproductive; indeterminate trees were mostly small.

Seed-trap evidence for masting was weak for *A. rubrum*: the serial correlation (using detrended series) for traps from stands having the longest collections of 11 years (C1–C5) were slightly negative, and they tended to be positive again at lags of two or three years (Fig. 4). All but the highest-elevation stand showed seed failure in 1996 followed by high production the following year (Fig. 3a). Year-to-year variation in *Acer* seed rain, summarized by coefficients of variation among years for the five stands, were 1.71, 0.79, 0.737, 0.954, and 1.10.

Parameter estimates

For *A. rubrum*, the fitted model consists of the joint posterior taken over 10 parameters (Tables 2 and 3),

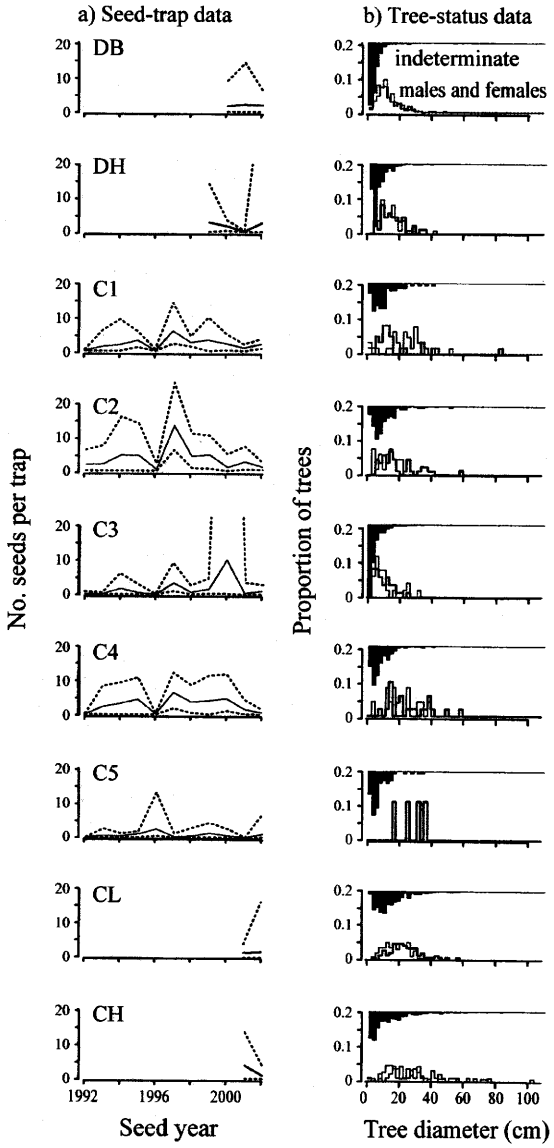

FIG. 3. Two types of data used in this analysis shown for *Acer*. (a) Mean seed rain for all traps (solid lines) and the range of observations (dashed lines). Stand codes are as in Table 1. (b) Frequency distributions for three kinds of tree status. Small trees tend to be indeterminate (solid histograms, upside down), because they are not mature. Large indeterminate trees tend to result from recognition failure. Trees identified as male (thin lines) or female (heavy lines) are shown as overlapping histograms.

4774 individual effects (β_i), and 22 172 latent seed production rates (y_{it}) for a total of 26 956 estimates. Likelihoods taken at the posterior mean show relative contributions of the two data sets to the fitted model. Visual summaries include comparisons of observed seed-trap counts s_{jt} plotted against predicted Poisson means $A_j g_j(y_t)$. The log plot (Fig. 5a) shows the low end of the scale, where most values lie, but, of course, omits traps that accumulated no seed in a given year. The linear plot includes these observations (Fig. 5b). A histogram of diameters identified as female is compared with the appropriate model prediction $\theta_i \phi v$, i.e., the probability of being mature, female, and correctly recognized as such (Fig. 5c). The complement, $1 - \theta_i \phi v$, is the total probability for trees identified as male or indeterminate.

Although all estimates are marginally dependent, many are most influenced by subsets of the data. The log likelihoods for the two data sets in Fig. 5 reflect not only the model fit, but also the relative amounts of tree years and trap years. For *A. rubrum*, there are far more tree years than trap years, as reflected in large log likelihoods for tree-status observations. This im-

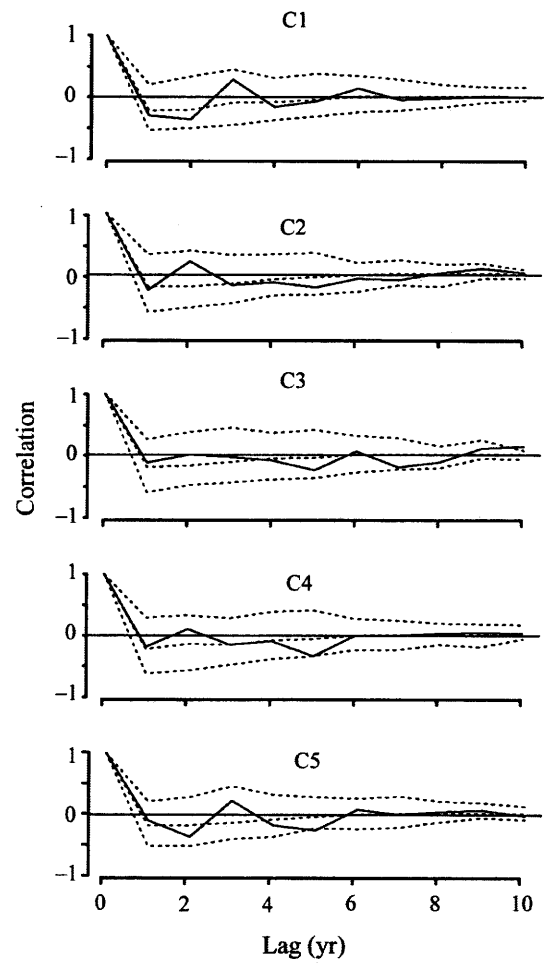

FIG. 4. Autocorrelation in seed-trap data (solid line) and in individual-tree fecundity estimates (dashed lines) for *Acer*. For trees, autocorrelations are taken for $\log_{10}$ posterior mean fecundity. The central dashed line is the median tree. The outer dashed lines bound 95% of the posterior means taken over all individuals. Series were detrended prior to analysis. Stand codes are as in Table 1.

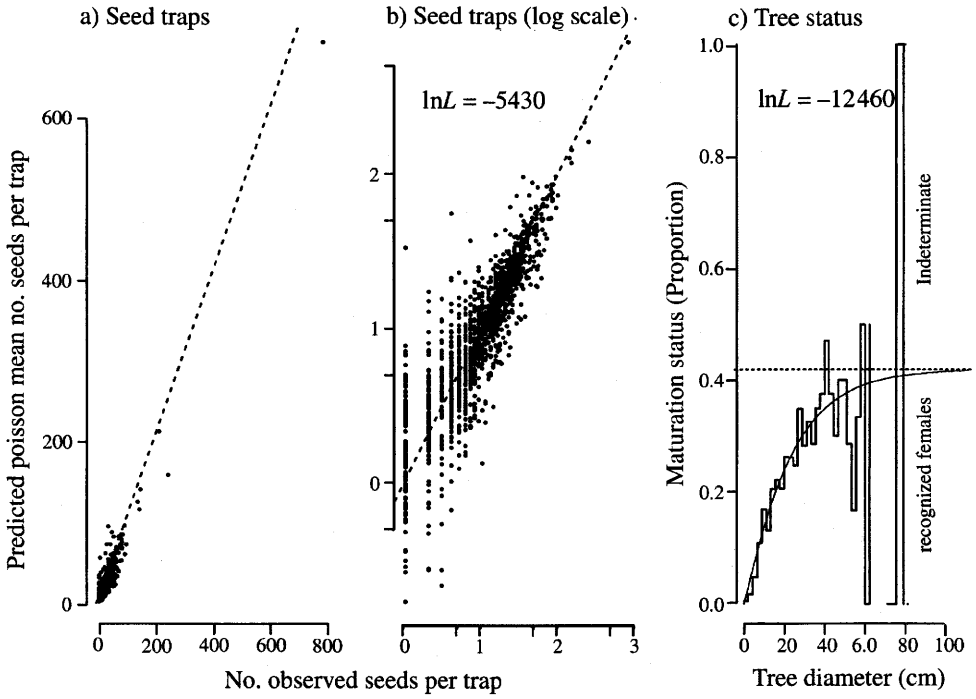

FIG. 5. Comparison of model predictions and observations for *Acer*. Panels (a) and (b) show seed-trap data [log–log plot in panel (b)], with each dot indicating an annual seed density for a given trap. (c) Tree maturation-status observations are summarized as histograms and compared with the fitted model $\theta\phi\nu$, the asymptote representing the product of female fraction ϕ and recognition success ν, and the sigmoid curve representing the maturation schedule θ. Log likelihoods for data sets are taken at the posterior mean.

balance of tree vs. trap information does not mean that tree data are the dominant influence on all parameters. Tree data have most direct impact on parameters describing maturation status, female fraction, and recognition error. The recognition error is strongly affected by the fraction of large trees that are assigned a particular status. The "asymptote" of the fitted status model shows this relationship (Fig. 5c). Seed data also affect this fit, but indirectly. For example, a seed trap that collects copious seed near an indeterminate individual lends support to the possibility that it is an unrecognized female. The probability of this tree-status observation is conditionally $\phi\theta(1 - \nu)$, so the estimates of ϕ and θ would tend to be increased by this observation, while the estimate of the recognition probability ν would tend to be reduced. Likewise, a trap that collects few seed near a recognized female would have larger effect on estimates of the dispersal parameter u and conditional fecundity y_{it} than would a tree of unknown status—we know it to be mature, so low seed accumulation is attributed to low production or limited dispersal.

While the widths of credible intervals for all parameters in Tables 2 and 3 asymptotically decline with sample size, those of the latent variables y_{it} do not. Estimates of a series $\mathbf{y}_i$ are not equally influenced by all traps, but rather by those nearby. Increasing the size of data set (adding more trees and traps) would be expected to change estimates of $\mathbf{y}_i$ only indirectly, by way of information those additional data confer on population parameters in Tables 2 and 3. With data sets as large as those used here, confidence envelopes on $\mathbf{y}_i$ are not expected to change appreciably with additional data.

Population parameters for most species are identifiable, as indicated by narrow confidence envelopes (Tables 2 and 3) and by weak parameter correlations, because data sets are large. For *A. rubrum*, a subsample of 120 evenly spaced Markov-chain Monte Carlo (MCMC) samples (to overstep inherent autocorrelation in the Markov chain) illustrates that only a_θ and b_θ ($r = 0.936$) showed strong correlation (Fig. 6). This correlation is expected, because they together determine the mean and variance of the cumulative gamma function θ. Unlike the normal distribution, the mean and variance for the gamma are not described by independent parameters. Thus, we would not draw independent inference on these parameters, but such inference is not our goal. The only other combination showing correlation, the regression parameters α_0 and α_1 ($r = -0.786$), is also reasonable as the natural tendency for a regression slope and intercept. Again, as independent

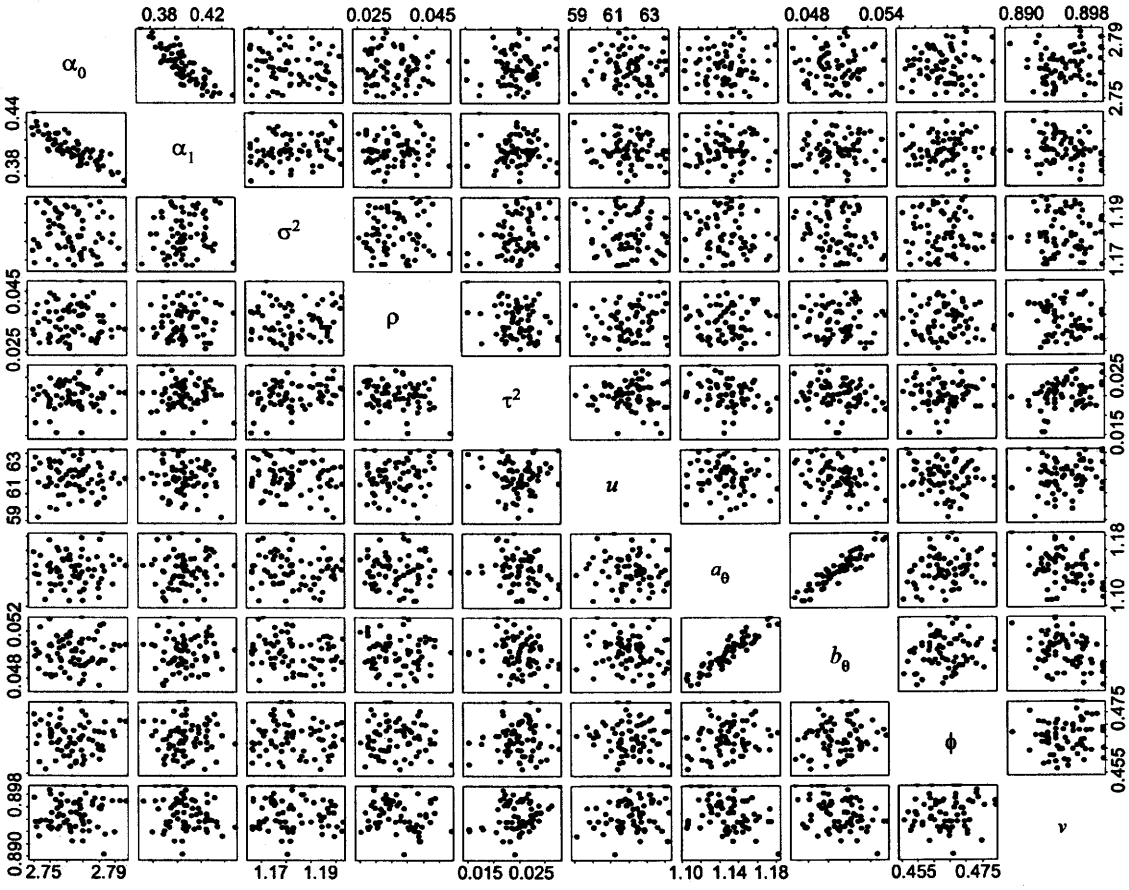

FIG. 6. A sample of Markov-chain Monte Carlo steps for all combinations of *Acer* parameters in Tables 2 and 3. Correlations are near zero for all parameter pairs except regression parameters (α_0 and α_1) and maturation parameters (a_θ and b_θ) (see *Results: Parameter estimates*).

inference on these parameters is not the goal, this correlation is not of great consequence.

Recognition success.—Recognition success ranged from 0 (no reproductive individuals were identified as such for *Robinia* and *Tilia*) to 90% (*Acer rubrum*)(Fig. 7b). In addition to *A. rubrum*, species tending to have high recognition success include *Betula* (conspicuous catkins), *Carya* (large nuts), and *Liriodendron* (carpels that persist into winter when foliage is absent). For the most part, low recognition success results from low seed production in dense stands (e.g., *Cornus*) or difficulty recognizing small- to moderate-size fruits in tall, dense canopies.

Female fraction.—Of the three dioecious species, *A. rubrum* data provided confident parameter estimates of female fraction, and *Fraxinus* and *Nyssa* data provided insight, but not confident estimates. *Acer* yielded confident estimates, because conspicuous red seeds and flowers made for easy recognition (Fig. 7b) and, thus, substantial numbers of male identifications. Females comprised nearly half the population (Fig. 7a). Because no male *Nyssa* trees were identified as such, we draw inference on the composite parameter $v\phi$, which has a posterior mean of 0.378, with a 95% CI of [0.316, 0.452]. Of 1305 *Nyssa* trees, 15 were identified as female. However, on large trees, fruits were obvious. If a large fraction of the indeterminate large trees are males, then the female fraction may be near 40%. For *Fraxinus*, $v\phi = 0.234$, with a 95% CI of [0.185, 0.282]. Of 808 trees, 22 trees were identified as female and 2 trees as male. Because *Fraxinus* seeds are not conspicuous, the estimate of $v\phi$ is heavily influenced by seed-rain data.

Maturation schedule.—Although maturation parameters showed positive correlation (see above), the ratio a_θ/b_θ is identifiable (Fig 7c), and varied widely among species. This ratio represents the diameter at which the cumulative gamma function is equal to 0.5, but it is not the diameter at which half the population is reproductively mature. Moreover, this is a "population-level" parameter. Because random individual effects are included in the regression for y_{it}, there is no need to

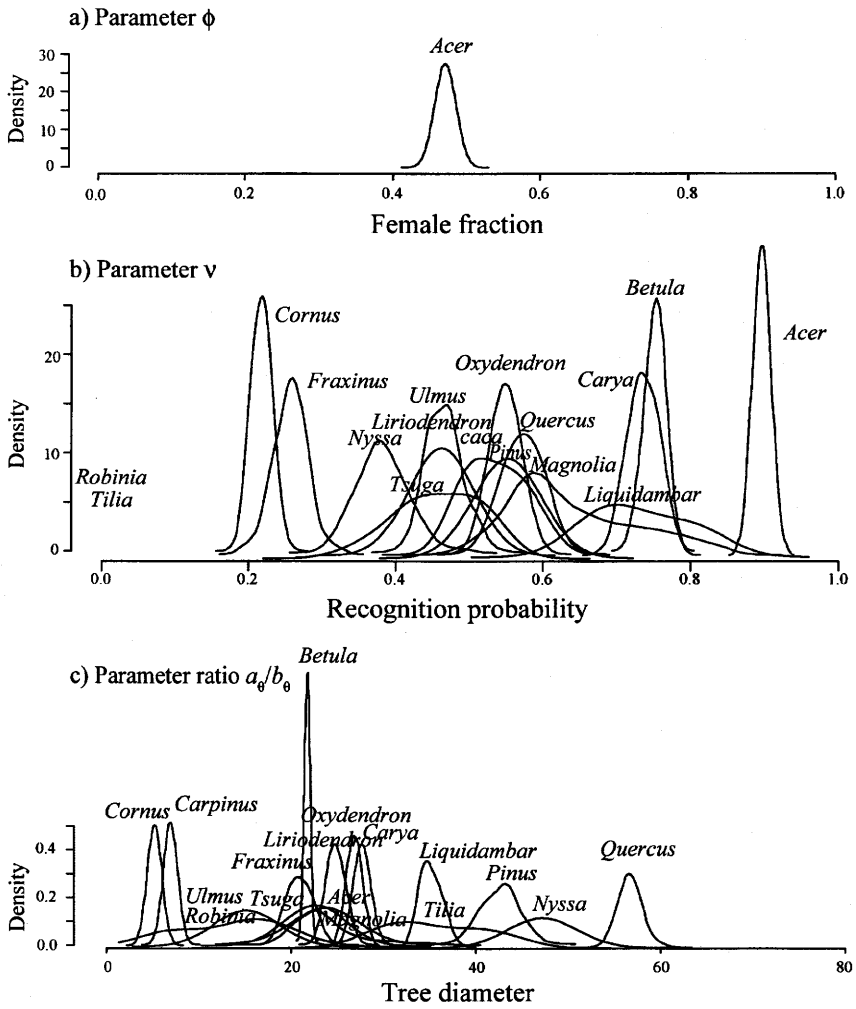

FIG. 7. Marginal posteriors for (a) female fraction, (b) recognition success, and (c) the diameter at which the cumulative gamma function $\theta = 1/2$. The density for a parameter p has units of $1/p$ (vertical axis).

also include random individual effects in θ. The parameter θ has two roles. First, it allows individual-status observations as a multiplier for the conditional fecundity schedule y_{it}. Second, it adds flexibility to the diameter:fecundity relationship at small diameters. Parameter identifiability is important, but the precise values are of consequence only in terms of the product $F_{it} = \theta_{it} \times 10^{\nu_{it}}$.

Conditional fecundity.—The log regression parameters α_0 and α_1 describe the shape of the log-linear regression of seed production with diameter, having most influence as trees become large. The shape of the fecundity:diameter relationship for small trees is controlled primarily by θ; the smaller the diameter at which θ approaches 1, the smaller the diameter at which α_1 becomes influential. *Betula* and *Liriodendron* had high estimates of α_0 and, thus, tend to have high fecundity for a given diameter (Tables 2 and 3).

Most species had shape parameter estimates $0 < \alpha_1 < 1$ (Tables 2 and 3), indicating that, as trees become large, there is a tendency for seed production to "decelerate." Because of the large number of observations, estimates were not sensitive to prior parameter values. *Carpinus* and *Pinus* had estimates near 1, indicating weak tendency for fecundity to saturate at large diameters, whereas *Betula* had estimates near 0, indicating a tendency to saturate. Obviously, this parameter depends on the numbers of large trees in the data set. Although most trees are small, small trees do not control shape at large diameters. Small trees principally influence shape through θ. Thus, the shape parameter α_1 is sensitive to large trees.

Individual effects.—Species with high τ^2 estimates indicate individual differences in how fecundity changes with diameter. Although this parameter appears in the regression for conditional fecundity, it effectively absorbs individual effects on maturation, because θ is restricted to population effects. Individual effects are especially large for *Nyssa*, *Ulmus*, *Tsuga*, *Pinus*, and *Magnolia* (Fig. 8a).

Serial autocorrelation.—The year-to-year correlations in fecundity were identifiable and ranged widely among species (Fig. 8b), from extremely negative (*Liquidambar*, *Cornus*, *Betula*) to extremely positive (*Oxydendrum*). Detrended fecundity series for most species have negative lag-1 correlation.

Fecundity schedules: size and year effects

Posterior estimates for individual trees demonstrate large interannual variation. Posterior means for *Liriodendron* trees are shown at left in Fig. 9, with 95% confidence intervals for a random sample of five trees above. Across the full population over all years, ~95% of fecundities F_{it} are bounded by the 95% prediction interval for the population. This relation is represented in the lower left panel of Fig. 9 by the fact that most posterior mean values lie within the population prediction interval, PI. The range of variation is large: some estimates exceed 10^6.

The relative contributions of stochasticity sources are shown in Fig. 9b. The posterior median estimate of the diameter effect (solid line in Fig. 9b) is embedded within three pairs of dashed lines that bound different sources of stochasticity, each at the 95% level. The inner pair bounds the population mean response $\hat{F}_i = \hat{\theta}_i \times 10^{\hat{\alpha}_0+\hat{\alpha}_1 d_i}$, which takes cognizance of uncertainty in the parameter estimates α_0, α_1, a_θ, and b_θ. This interval is the closest analogy to the credible interval that would be constructed as part of a non-hierarchical model.

The second pair of dashed lines combines the parameter uncertainty for the mean responses with individual effects and describes population heterogeneity. This response is $\hat{F}_i = \hat{\theta}_i \times 10^{\hat{\alpha}_0+\hat{\beta}_1+\hat{\alpha}_1 d_i}$ where the variance includes that contributed by individual effects $\beta_i \sim \mathcal{N}(0, \hat{\tau}^2)$. The individual effects are also shown (short solid lines) to indicate how each tree contributes to the overall fit.

The outermost pair of lines is the 95% PI for the full response, including process misspecification, i.e., $\beta_i + \varepsilon_i \sim N(0, \hat{\tau}^2 + \hat{\sigma}^2)$. This is the combination of individual effects, parameter uncertainty, and process variability, and it constitutes the prediction interval (PI) for fecundity of a tree and year selected at random (Eqs. 19 and 20).

The sources of stochasticity constitute differently to fecundity schedules. For this example, parameter uncertainty is small, because we have large data sets. This low parameter uncertainty translates to a narrow PI on the mean fecundity process for a given diameter tree $\hat{F}$. The narrow PIs do not mean that we can expect informative predictions for a random tree and year, because there are larger year-to-year effects, included in σ^2, and large individual variation τ^2.

Plotted by year, the variation for *Acer* shows patterns of synchronicity for subsets of the population (Fig. 10: upper panels). The crop failure in 1996 observed in seed traps (Fig. 3) applies to the full population (Fig. 10). The exception at stand C5 results from *A. saccharum*—most trees of this species occur on C5, and three trees on this plot had high seed production in 1996. Few *A. rubrum* individuals had good seed years two years running. Most experienced high fecundity in 1997, suggestive of reserves available that year due to low production the year before. Any synchronizing effect this event may have had appears to have been transient. The additional series that appear in 2000 and 2001 represent stands added that year (stands CL, CU, DB, and DH, Table 1).

The degree of synchronicity among individuals is illustrated by a histogram of pairwise correlations (Fig. 11). While synchronicity among a substantial part of the population is high (e.g., >0.6), much of the population behaves more-or-less independently (the mode of the histogram is near 0). The synchronized individuals are not necessarily the largest ones. We found no tendency for high correlations to be clustered at high diameters.

Plotted against diameter, individual fecundity series show how the diameter effect is obscured by individual differences and interannual variation (Fig. 10: lower panels). The excursions to high values are emphasized in this figure, because the dominant low values overlap. The dashed lines in the lower panels of Fig. 10 show the upper bound of the 95%PI for fecundity; 2.5% of all values lies above this line. Thus, a relatively small number of years dominate the total seed rain.

Although populations vary in terms of their levels of heterogeneity, on balance, within-population variability tends to be large (Fig. 12). For many species the variability among individuals of similar diameter spanned more than an order of magnitude; some individuals contribute disproportionately to overall fecundity. For example, *Nyssa* had an estimate of τ^2 nearly half as large as σ^2, and, for *Ulmus*, they were approximately equal (Tables 2 and 3). *Ulmus* estimates come from relatively short 3- and 4-yr data sets. Larger data sets might reduce the estimate of within-population variability. Nonetheless, even within heterogeneous populations, random effects of individuals (summarized by τ^2) tend to be smaller than process variance σ^2. For most species σ^2 is one to two orders of magnitude larger than τ^2 due to year-to-year variability (Fig. 12).

Species relationships

The large interannual variability described by σ^2 and, to a lesser degree, population heterogeneity τ^2, means

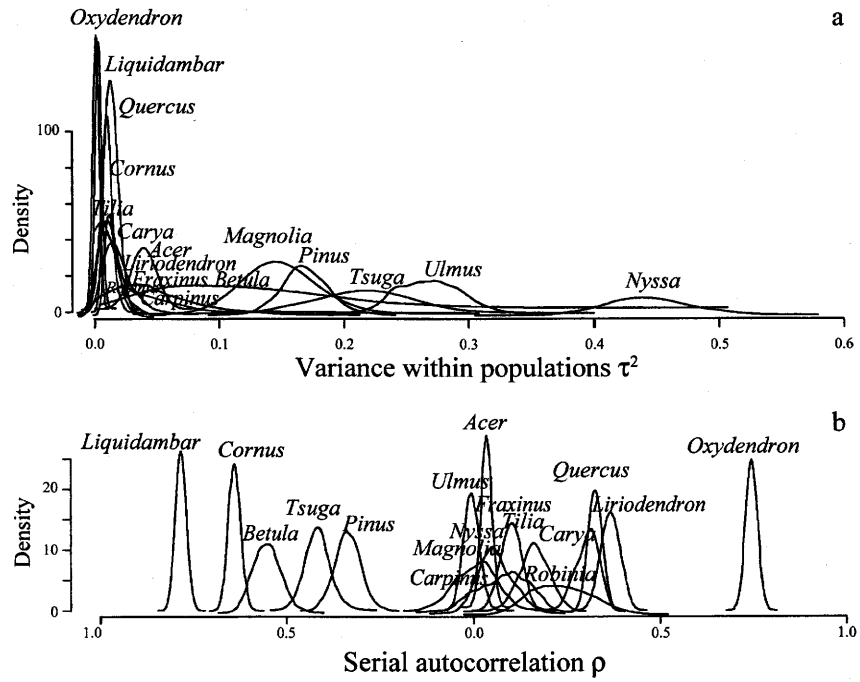

FIG. 8. Marginal posteriors for (a) individual effects (τ^2) and (b) serial autocorrelation (ρ). The density for a parameter p has units of $1/p$ (vertical axis).

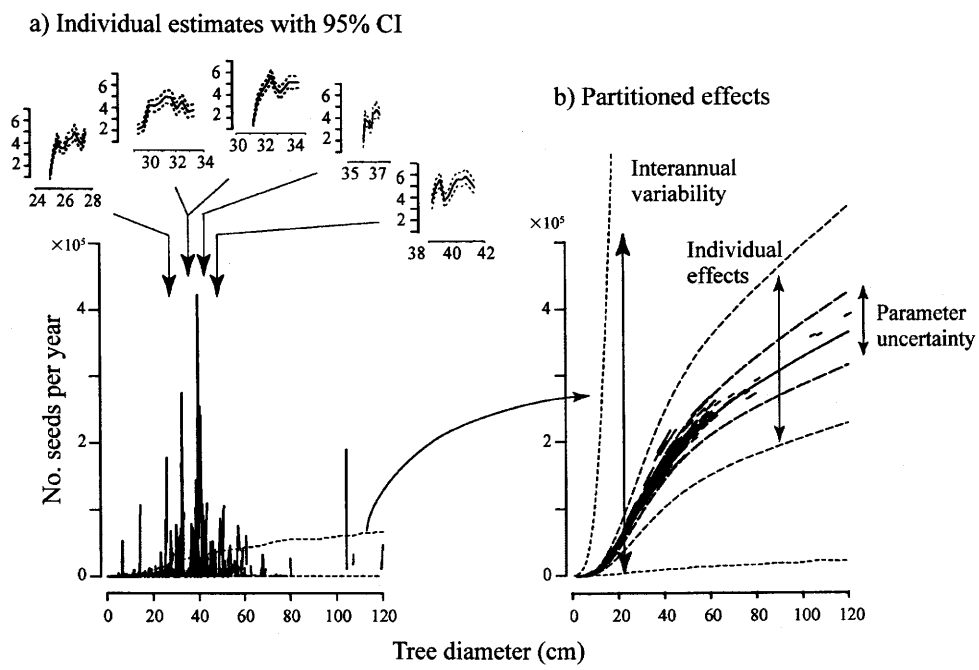

FIG. 9. Posterior log fecundity series for five randomly selected *Liriodendron* individuals (a, top), together with the full set of *Liriodendron* fecundity values (linear scale) plotted against diameter (a, bottom). (b) The 95% confidence intervals for three sources of stochasticity. The population "mean" response (solid line) is bounded by the inner 95% confidence intervals that integrate uncertainty in all parameters describing the mean response, including α_0, α_1, μ, a_θ, b_θ. "Individual effects" incorporate the additional variability that comes from differences among trees (τ^2). Interannual variability dominates the "process error" (σ^2) and is represented by outer 95% confidence intervals.

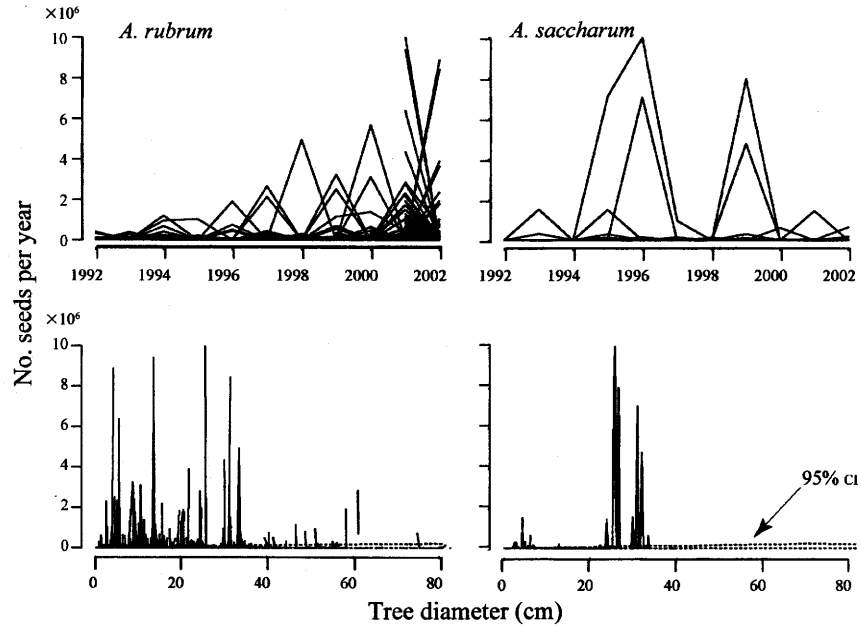

FIG. 10. Posterior mean individual fecundities plotted by year (upper graphs) and by diameter (lower graphs) for *Acer*. Credible intervals for individual years are omitted, but examples are included for *Acer* in the Appendix. There is one curve for each of the 4774 trees. Dashed lines on the lower panels bound 95% credible intervals.

that fecundity schedules (Fig. 12) and seed shadows of different species broadly overlap (Fig. 13). This large variability overwhelms differences in fecundity among sites. We constructed full fecundity schedules for all plots, but none showed appreciable differences. There are three implications. First, this broad overlap in Fig. 13 does not indicate that there are no differences among species. A traditional interpretation of the confidence envelopes might lead us to say that species "are not significantly different." The wide prediction intervals here include variability, not just parameter uncertainty. Despite broad overlap, large populations will explore these different envelopes, so the traditional concept of "significance" is not appropriate here.

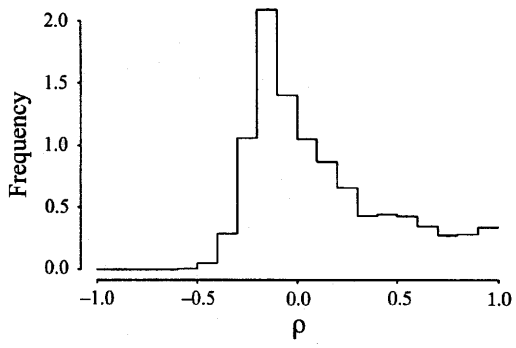

FIG. 11. A histogram of pairwise correlations among trees for plot C1, illustrating the degree of synchronicity among individuals.

Second, a typical reaction to wide confidence envelopes is to conclude that we have no information. The "true" value might lie anywhere within the envelope, so we can infer little from the analysis. Again, this interpretation would be misguided. The prediction intervals reported here inform us about population variability. We have confidence in the fits themselves, to the extent that parameters are identifiable (Tables 2 and 3). But the mean response does not summarize the population heterogeneity, which overlaps broadly among species.

In light of the first two points, the third implication is that within-population variability tends to overwhelm differences in species mean responses. Moreover, there is no tendency for the combined effects of fecundity and dispersal to suggest that colonization is related to successional status (Fig. 13).

Evaluation

We cannot evaluate results using direct comparisons with seed production, because direct counts would require a destructive harvest before seeds are released (Fig. 1). Insights are available from comparisons involving several lines of evidence and from other methods. The method of scaling densities of seeds in traps by crown area does not account for effects of dispersal, and it is difficult to obtain large sample sizes. It does provide a rough guide for seeds that have limited dispersal. A study from the southern Appalachians (Greenberg and Parresol 2002) reports average esti-

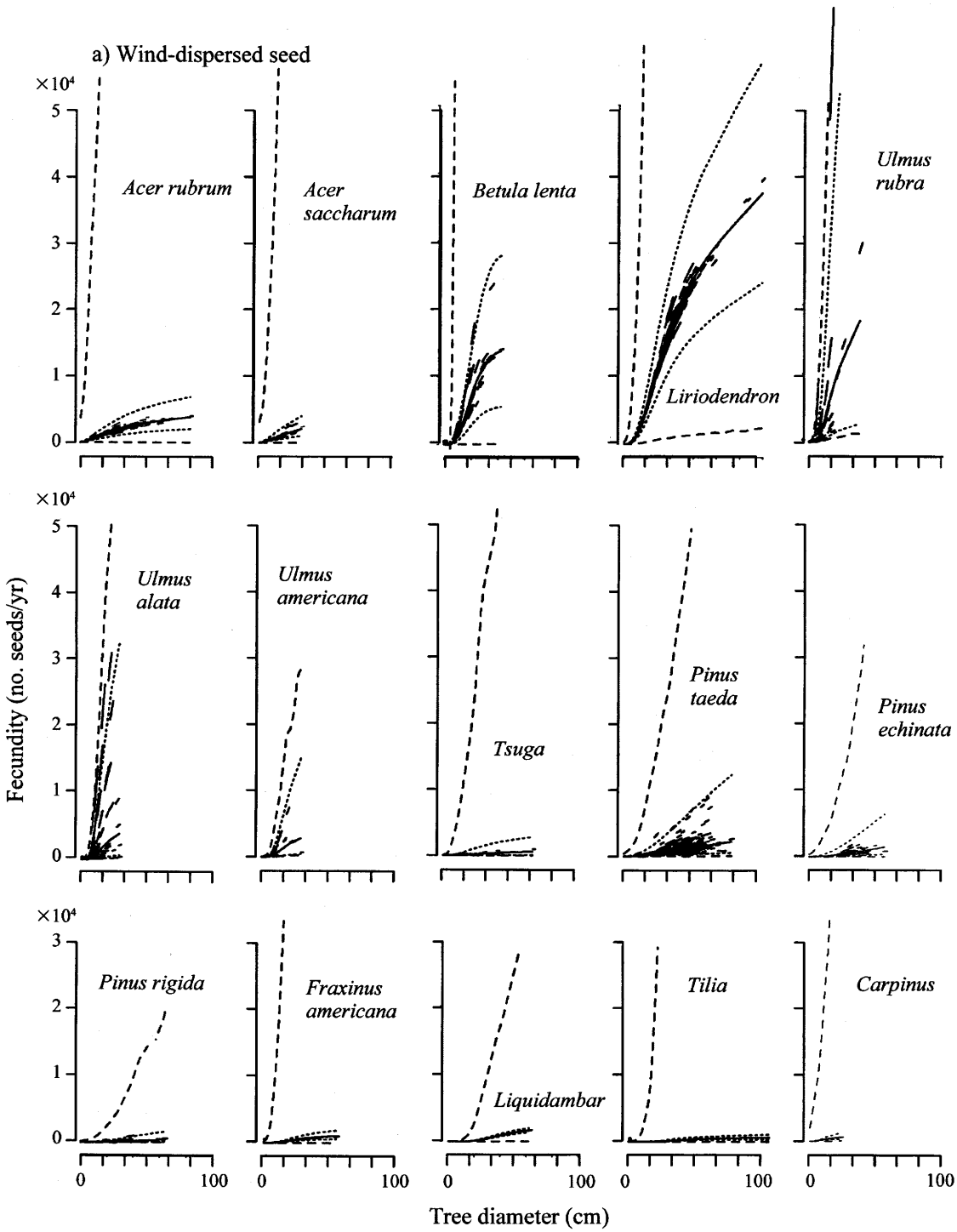

FIG. 12. Fecundity schedules for (a) wind-dispersed and (b) animal-dispersed taxa showing posterior means (solid lines) and 95% prediction intervals for individual effects (interior dashed lines) and process variability (outer dashed lines).

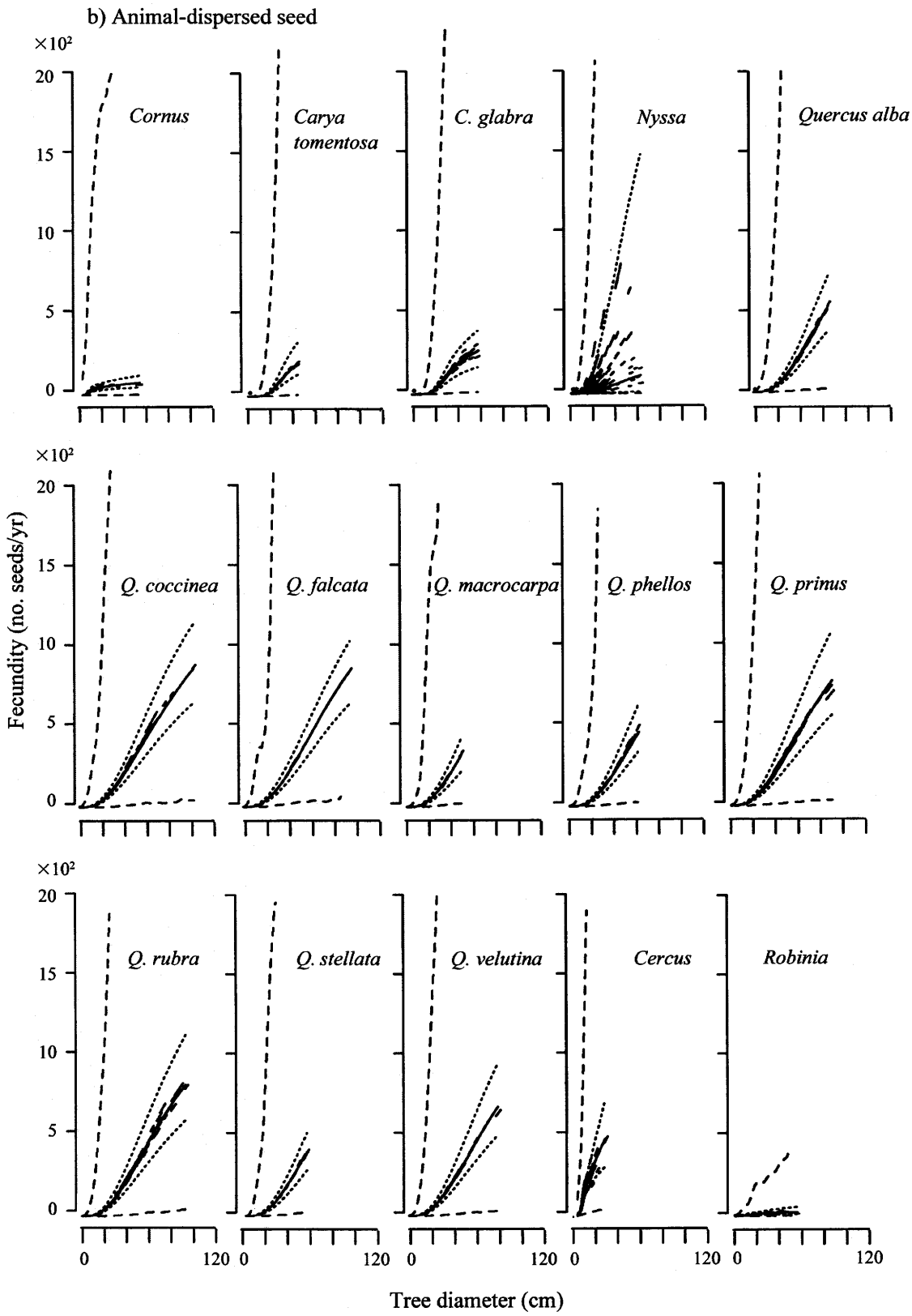

FIG. 12. Continued.

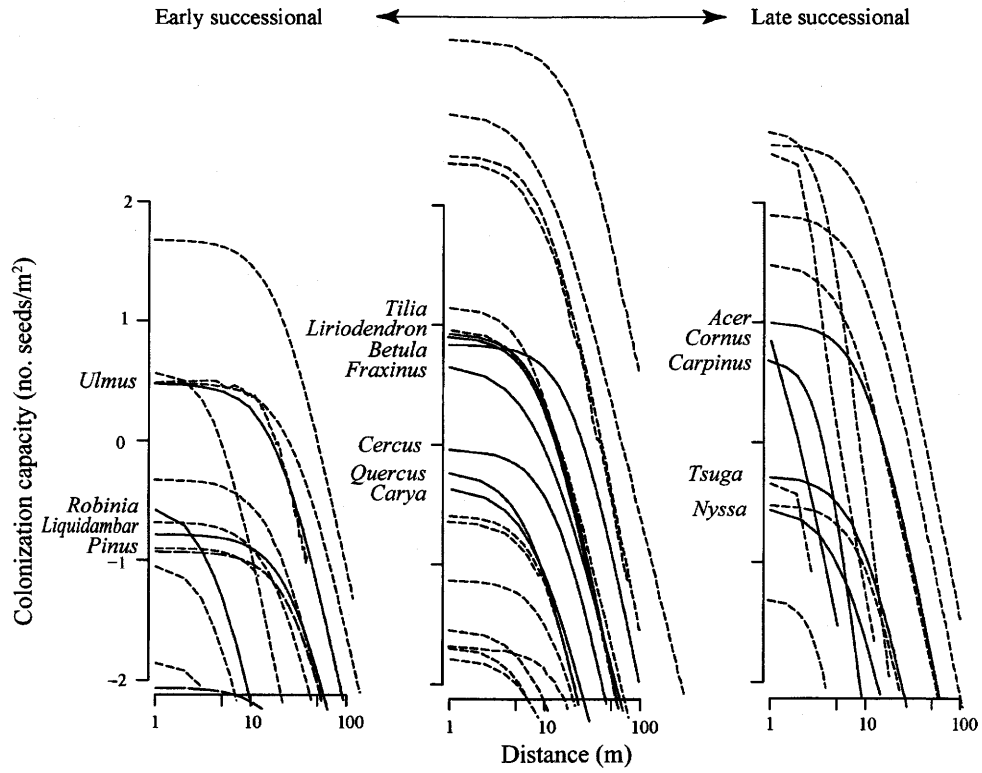

FIG. 13. Colonization capacity, as influenced by the number of seeds dispersed over distance by a 25 cm diameter tree. The 95% prediction intervals are for parameter uncertainty plus individual effects (inner dashed lines) and with process variability (outer dashed lines). Note x-axis logarithmic scale.

mates for oak species included here (Fig. 14). White oak had especially high estimates of fecundity, F, per squaremeter of basalarea, B: $F/B = 4216$ seeds/m^2. Remaining species ranged from $F/B = 1274$ to 2807 seeds/m^2. In these units we obtain estimates of $\hat{F}/B = \theta\,(d;\,\hat{a}_\theta,\hat{b}_\theta) \times 10^{\alpha_0+\alpha_1 d}/B = \hat{\theta} \times 1052B^{-0.715}$; the last step comes from converting d (in centimeter) to B (in square meters) and inserting parameter estimates from Table 2. For relevant diameters we obtain values of 1485 seeds/m^2 (a 70-cm tree) to 1627 seeds/m^2(a 30-cm tree), which fall in the center of the range estimated by Greenberg and Parresol (2002) for the red oak group (our plots contained few white oaks). By contrast, the maximum-likelihood (ML) approach of Clark et al. (1999*b*) produces estimates of 5260 to 60 800 seeds/m^2 basal area, values that both this analysis and Greenberg and Parresol's (2002) data suggest are up to two orders of magnitude too high (Fig. 14). The classical analysis of Clark et al. (1999*b*) only includes the first six years of data used in our analysis, but the longer data set included here does not explain our lower fecundity estimates, as the early years did not have substantially lower seed rain than the additional years included here.

The large overestimates of fecundity obtained by previous ML approaches probably apply to all species examined here. They derive from inflexibility of the one-parameter fecundity schedule and inappropriate treatment of stochasticity in this nonlinear model. The flexible model that results from integrating the saturating maturation status θ with the log-linear conditional fecundity schedule allows for the steep rise in seed production at small diameters, where most of the data lie, and for the tendency to slow at larger diameters. Fits are dominated by the large numbers of small trees that describe exponential increase with diameter that does not apply to large trees.

Inappropriate treatment of stochasticity affects parameter estimates. Because the traditional method could not accommodate lognormal variation at the level of individuals, it is strongly affected by high seed years. The relatively infrequent high seed years inflates the estimate of mean fecundity. Our lognormal stochasticity on conditional fecundity and individual effects provide for these excursions. For example, the estimate of 10^6 seeds on a single red maple tree (Fig. 1) is fully compatible with our model for specific individuals and years (Fig. 10), but it is orders of magnitude higher

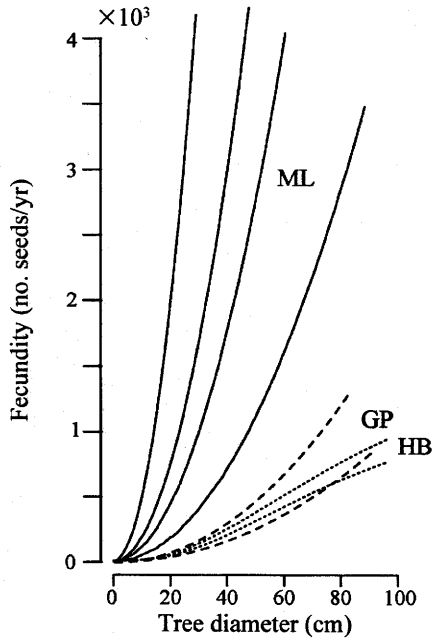

FIG. 14. Comparison of fecundity schedules obtained here (HB, dotted lines) with those from a maximum-likelihood, (ML, solid lines), approach (Clark et al. 1999*b*), and traps below isolated trees (GP, dashed lines; Greenberg and Parrasol 2002). Dashed lines are 95% confidence intervals that result from parameter uncertainty in population-level parameters. The ML method shows predicted mean responses for four different stands used in this study. Parameter uncertainty is the only source of stochasticity in the fecundity schedule using the classical method. The bias from previous methods results, in part, from inflexibility (see text).

than the mean response (Fig. 12). Using hierarchical Bayes we obtained fecundity estimates much lower than those using the classical model for all species (Clark et al. 1999*b*).

Not only fecundity, but also dispersal parameters (u) appear to be overestimated by previous classical methods. In this analysis, estimates of u are typically much lower than those obtained by the classical method of Clark et al. (1999*b*), suggesting that proper treatment of stochasticity is necessary.

DISCUSSION

Contrary to the colonization–competition hypothesis, which postulates a specific relationship between successional status and colonization ability, we find both no such trend and broad species overlap (Figs. 12 and 13). Our results do not show strong evidence for trade-offs that might derive from a combination of colonization–competition and successional niches. Our results suggest a mechanism that may be more general. We focus on two assumptions of theoretical models that our results demonstrate to be unrealistic, i.e., that individuals are identical, and that process variability can be ignored. We emphasize the widely appreciated fact that variability can be a key ingredient for coexistence, with estimates of variability within populations (τ^2) and over time (σ^2) that is unrelated to the standard explanatory variables. This variability dominates not only colonization (Fig. 13), but also competition (Clark et al. 2003).

Populations persist if gains offset losses. High diversity is possible for groups of species with long lifespans and variable recruitment, provided that recruitment is not closely correlated among species (Comins and Noble 1985, Warner and Chesson 1985, Chesson 2000, Hixon et al. 2002). Disproportionate gains during episodes that favor recruitment can offset low mortality losses of long-lived adults. Variability is not enough to promote coexistence. Species differences (trade-offs) are implicit for this "storage effect," because lack of differences means high correlation in how they respond to variability. If one species is always more successful than another species under one set of circumstances, coexistence requires alternative circumstances where others can succeed. The challenge comes in identifying the ways in which species can be sufficiently different to ensure that these correlations are weak, so that variability shifts the advantages among species.

Our results highlight the role of random individual and temporal effects (RITEs). It is illustrated with an example of two species that coexist in both of our study regions, but we could have chosen others. Consider first the classical approach. We might begin by parameterizing recruitment capacity (Fig. 15: upper left) and response to a common limiting resource, e.g., light (Fig. 15: upper right) (Clark et al. 2003). The fitted model from such an analysis shows that *Liriodendron* has the growth advantage at all light levels. As long as light is the variable that limits success, *Liriodendron* will dominate. Because *Acer* is not rare, we search for other circumstances in which it can dominate. For colonization, we find that it has a higher capacity to reach sites nearby than does *Liriodendron*, but *Liriodendron* still has the advantage at most distances beyond the immediate canopy of the parent (Fig. 15, upper left). It has higher fecundity than *Acer* and, by virtue of high success at distance, may even obtain many sites near parent *Acer* trees. So it still does not look good for *Acer*. Clearly, we can continue in this fashion, searching for circumstances where *Acer* has the upper hand. There are many possibilities beyond those included in Fig. 15. Because all species truly are different, it is likely that only by giving up too soon will we fail to identify those circumstances. Once we find them, they can be our explanation for coexistence. Regardless of what they are, we can agree that they will contribute. For example, we estimate higher low-light survival for *Acer rubrum* than for *Liriodendron* (Beckage and Clark 2003), and this relationship appears important in diversity of northeastern temperate forests (Pacala et al. 1996).

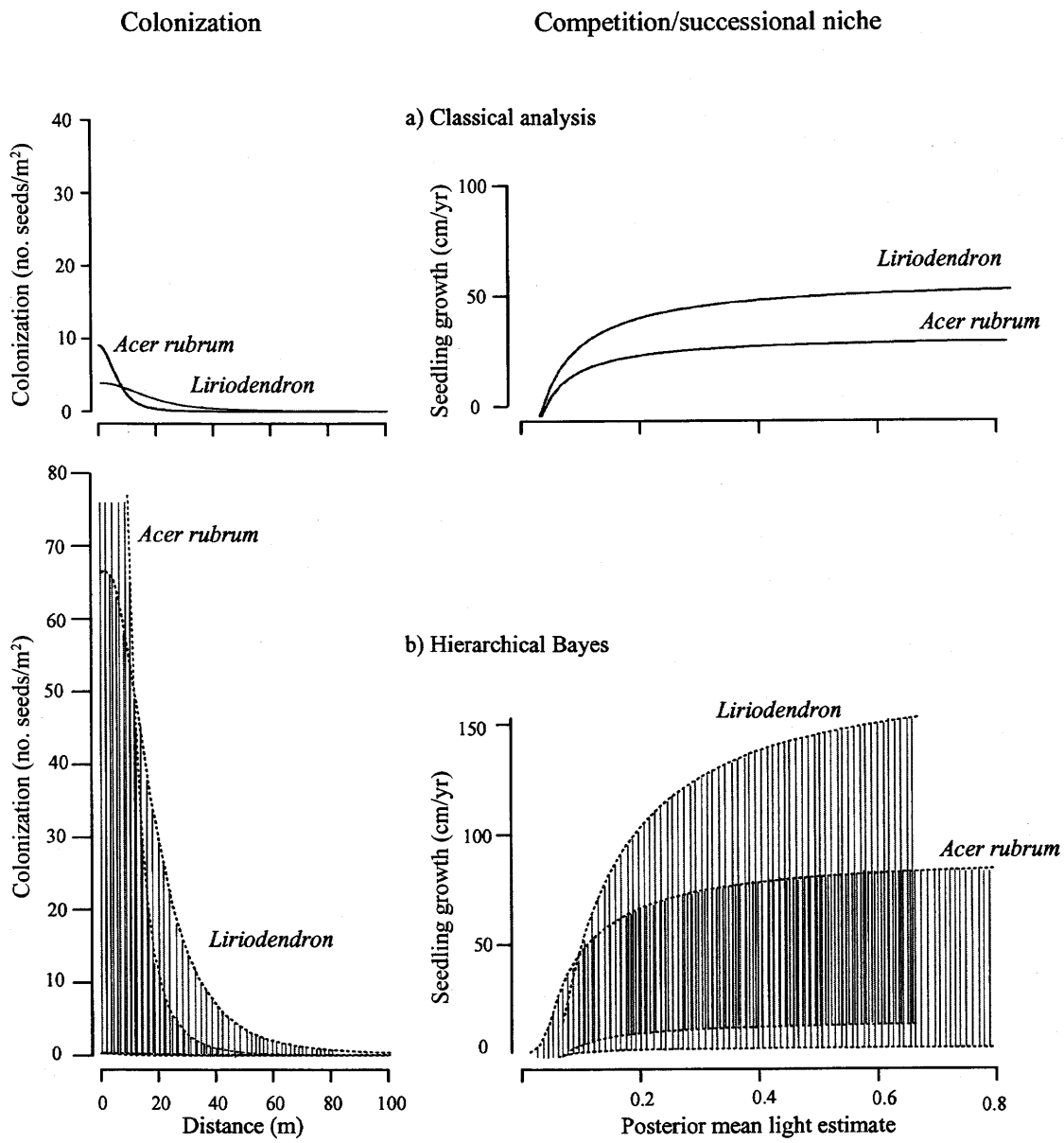

FIG. 15. Comparison of tree species coexistence using traditional model estimates (top panels) and with hierarchical Bayes (bottom panels). Dashed lines bound 95% confidence intervals that include process variability and individual effects. In panel (b), *Acer rubrum* has greater colonization at shorter distances (leftmost distribution). In (b), areas of overlay between the two species appear dark.

We speculate that RITEs might contribute to diversity regardless of whether or not *Acer* ever has the average upper hand. We find large variability in terms of which species has the advantage due to population heterogeneity (random individual effects) and large temporal variability. For example, our model predicts that seed densities near a tree, for a tree and year selected at random, can range from 0 to >100 seeds/m² (Fig. 15: lower left). Observations show these predictions to be accurate; even beneath trees of species with high average fecundities we may collect no seeds in many traps for a given year and a given individual. Much of the variability in fecundity is subsequently damped, because recruitment of many species will be unsuccessful at low light. In other words, the correlation among species, in terms of recruitment success,

will be greater than the correlation we observe in seed production. Nonetheless, the importance of "good seed years" for successful establishment is well known, and the massive stochasticity described by variance σ^2 (Table 2) combined with low correlation among species may contribute to diversity.

The contribution of random temporal effects may be less efficacious than that of random individual effects, which have prolonged impacts—populations consist of individual differences that persist throughout the lifetime. At a given light level, large variability within populations makes for broad overlap among species (Fig. 15: lower right)(Clark et al. 2003). We do not need to search for new axes where *Acer* has a deterministic advantage, because *Acer* can often have an advantage along the axes we have already examined. For both colonization–competition and successional niches, random effects at the individual level and process variability over time (RITEs) provide a massive source of stochasticity that can have low correlation among species at any given time and place. This stochasticity is not explained by additional resources that could have been measured, but were not included in the model. For example, soil moisture did not account for the broad overlap in light responses shown in Fig. 16 (Clark et al. 2003). Pacala et al. (1996) did not include nutrient availability in their model, because it did not explain recruitment patterns. We are now examining this mechanism in simulation (J. S. Clark, M. Dietze, S. Govindarajan, and P. Agarwal, *unpublished manuscript*).

The potential stabilizing effect of RITEs, seemingly without trade-offs, does not imply that it occurs in few dimensions. The massive process and population-level stochasticity parameterized here stands in for processes that are unknown, not measurable, or both (Clark et al. 2003). Instead, these results demonstrate that low-dimensional models based on variables that are readily measured (resource responses, life history, and so forth) may not make the dominant contribution to coexistence. They will often be overwhelmed by factors that are not measurable and, unless properly accommodated by inference, not accurately represented in ecological models. If we could know and quantify all factors that contribute stochasticity, the model would be deterministic, and it would involve many dimensions that describe how individuals differ and environments vary.

Nor does this explanation imply that trade-offs play no role in coexistence. Long-recognized differences between early- and late-successional species (Connell and Slatyer 1977, Huston and Smith 1987, Wright et al. 2003) support the notion that the successional niche explains coexistence of these two "classes" of species (Pacala and Rees 1998, Bolker and Pacala 1999). Beta diversity across landscapes depends on some clear physiological adaptations to moisture availability, drought, and nutrients (Pastor et al. 1987). On the other hand, these attributes may not be sufficient to explain coexistence of species that share late-successional habitats or that share specific soil types (i.e., alpha diversity). The large stochasticity in terms of RITEs that we parameterize may contribute.

The broad overlap we find is not expected to cause "neutral drift." Random effects illustrated in Fig. 16 might seem like "equalizing mechanisms" (Chesson 2000), because they seem to increase similarity among species and, thus, should slow competitive exclusion (Hubbell 2001). If intraspecific variability does promote coexistence by spreading the advantages among individuals, this effect could be "stabilizing" by promoting diversity, rather than simply slowing its decay. Our results may help to square the observation that dynamics show stability (Clark and McLachlan 2003) with the observation that trade-offs are often not apparent (Hubbell 2001).

The contribution of RITES can be overlooked due to their omission at the two critical stages. First, theoretical models do not include them. Many ecological models admit stochasticity. Individual-based models have stochastic births and deaths (individuals are discrete), but demographic stochasticity is more restricted and operates differently than the variability estimated here. For example, models that allow demographic stochasticity do not include variability in how individuals in a given state (size, age, location, . . .) respond. They are "individual-based" models, but they do not allow random individual effects.

Ecological models that do not track individuals are often implemented with stochastic parameters with interannual variability. The assumption of noise in a parameter that is drawn each time step and applied to the full population does not allow for the differences among individuals that causes broad overlap. Random individual effects are structured in a different way, because there are advantaged and disadvantaged individuals that remain so throughout out their lifetimes.

It is impossible to identify the mechanism when it is assumed not to exist. The stochasticity parameterized in Fig. 15 is not parameter error. Pacala et al. (1996) introduced to stand simulators the important concept of "error analysis" (Lande 1988). However, parameter error is an insignificant contribution to the processes we estimate. Moreover, unless sample sizes are small, that parameter error is small relative to individual effects and process variability (Fig. 11 and Clark et al. 2003), and it has a different structure. Parameter error is an important consideration (e.g., we incorporate that here with other sources of stochasticity), but it does not address variability in the process or misspecification of the model.

Theory that lacks random individual effects is only part of the reason this simple mechanism has been overlooked. The second critical stage involves the statistical models used to estimate life histories and trophic relationships. Empirical studies have not parameterized

the massive contribution of RITEs, because models that include them are not amenable to classical methods (see also Clark 2003, Clark et al. 2003). Most careful studies of seed production note this large variability among individuals and years (e.g., Downs and McQuilkin 1944, Koenig and Knops 2000, Greenberg an Parresol 2002). That stochasticity is not transferred to models that ecologists use to evaluate mechanisms of coexistence. Even for simple deterministic processes, inference can entail high-dimensional models. This high dimensionality leads us to mention several other aspects of model complexity.

So many parameters?

Clark et al. (2003) point out that most sources of variability in many ecological data sets will be unknown. This reality motivates models that have few deterministic elements. The deterministic elements of our fecundity model include only tree size and dispersal (Fig 2). Nonetheless, the sources of variation that go beyond these relationships cannot be ignored (e.g., Fig. 14). To accommodate the factors that impact data on fecundity schedules required nearly 10^5 parameter estimates. The high dimensionality was needed to allow for the unknowns, such as sampling errors, and observation errors, and variability in fecundity that is related to year and time. To estimate 10 parameters related to fecundity for a given species, we also had to estimate seed production by every tree, every year. Obviously, there is a trade-off in terms of deterministic process and stochasticity. Deterministic relationships are desired for the quantifiable relationships. Stochasticity allows us to accommodate the ones that cannot be measured. Hierarchical Bayes provides a common framework. Such high-dimensional models will inevitably become more common in the environmental sciences. For example, weather prediction models can require 10^6 parameters (e.g., Bengtsson et al. 2003).

Uncertainty in fecundity schedules

Our estimates of recognition success near 50% (Fig. 7) are consistent with Chapman et al.'s (1992) evidence that variation among observer seed counts in tree crowns is large. Our results contrast with short-term observations that have been used to parameterize simple allometric relations between tree diameter and reproductive output—counting errors are large (Fig. 7), there is large fluctuation from year to year (Fig. 10) and among individuals (Figs. 11 and 12), and the allometric relationship itself changes with tree size. Size–fecundity relationships reported for tropical trees (e.g., Thomas 1996) may yield distinctive patterns because variability is muted there. Some authors suggest that seed production may be more variable at low latitudes (e.g., Koenig and Knops 2000). These apparent regional differences can be resolved if future studies estimate recognition errors as part of the analysis, which is straightforward with our approach (Fig. 7).

Population variation

Patterns of temporal variability in seed production are the basis for hypotheses regarding masting. Common indices include coefficients of variation among years (e.g., Kelly 1994, Herrera et al. 1998, Kelly and Sork 2002) and serial autocorrelation (Koenig and Knops 2000). A full time-series analysis of posterior fecundity estimates is beyond the scope of this paper, as it involves nearly 10^5 estimates (it is taken up elsewhere). Here we simply point out two general considerations. First, previous analyses of seed density (e.g., in seed traps) will find substantially less variability than occurs for the trees themselves due to the spatial averaging of overlapping seed shadows. Although the coefficients of variation we find for seeds are similar to those reported for other studies, we find that the year-to-year variability for individual trees spans several orders of magnitude (Figs. 9 and 12). Similar large variation has been estimated from direct seed estimates (Koenig et al. 1994). Large potential differences that have motivated the search for "bimodality" (e.g., Herrera et al. 1998, Koenig and Knops 2000) are consistent with large eruptions that are characteristic of all species we analyzed (Fig. 10).

Second, high interannual variation combined with large individual variation means that effective population sizes are often small and highly dynamic. We further find that masting does not engage the full population. While many individuals are roughly synchronized, other individuals and subsets of populations are out of phase. Effective population sizes range widely from year to year. Our model predicts Sharp's (1958) view that, even during mast years, only a subset of the population may produce a large seed crop. Interannual and individual posterior fecundity estimates provide a basis for a full analysis of effective population sizes and how they shift in space and time (J. S. Clark, M. Dietze, S. Govindarajan, and P. Agarwal, *unpublished manuscript*).

Acknowledgments

For comments on the manuscript and discussion we thank B. Bolker, M. Dietze, A. Gelfand, M. Hersh, J. McLachlan, J. Ver Hoef, M. Wolosin, and an anonymous reviewer. Research support was provided by NSF grants DEB-9632854 and DEB-9981392 and DOE grant 98999.

Literature Cited

Abbott, H. G. 1974. Some characteristics of fruitfulness and seed germination in red maple. Tree Planter's Notes May: 25–27.

Adler, F. R., and J. Mosquera. 2000. Is space necessary? Interference competition and limits to biodiversity. Ecology **81**:3226–3232.

Armstrong, R. A. 1976. Fugitive species: experiments with fungi and some theoretical considerations. Ecology **57**: 953–963.

Beckage, B., and J. S. Clark. 2003. Seedling survival and growth of three forest tree species: the role of spatial heterogeneity. Ecology **84**:1849–1861.

Bengtsson, T., C. Snyder, and D. Nychka. 2003. Toward a nonlinear filter for high-dimensional systems. Journal of Geophysical Research **108**(D24):8775.

Bolker, B. M., and S. W. Pacala. 1999. Spatial moment equations for plant competition: understanding spatial strategies and the advantage of short dispersal. American Naturalist **153**:575–602.

Carlin, B. P., and T. A. Louis. 2000. Bayes and empirical Bayes methods for data analysis. Chapman and Hall, Boca Raton, Florida, USA.

Caswell, H., and J. E. Cohen. 1991. Disturbance, interspecific interaction and diversity in metapopulations. Pages 193–218 *in* M. Gilpin, and I. Hanski, editors. Metapopulation dynamics: emphirical and theoretical investigations. Academic Press, London, UK.

Chapman, C. A., L. J. Chapman, R. Wangham, K. Hunt, D. Gebo, and L. Gardner. 1992. Estimators of fruit abundance of tropical trees. Biotropica **24**:527–531.

Chesson, P. 2000. Mechanisms of maintenance of species diversity. Annual Reviews of Ecology and Systematics **31**: 343–366.

Christensen, N. L., and R. K. Peet. 1984. Convergence during secondary forest succession. Journal of Ecology **72**:25–36.

Clark, J. S. 2003. Uncertainty in population growth rates calculated from demography: the hierarchical approach. Ecology **84**:1370–1381.

Clark, J. S., B. Beckage, P. Camill, B. Cleveland, J. Hille Ris Lambers, J. Lichter, J. MacLachlan, J. Mohan, and P. Wyckoff. 1999*a*. Interpreting recruitment limitation in forests. American Journal of Botany **86**:1–16.

Clark, J. S., M. Dietze, I. Ibanez, and J. Mohan. 2003. Coexistence: how to identify trophic trade-offs. Ecology **84**: 17–31.

Clark, J. S., E. Macklin, and L. Wood. 1998. Stages and spatial scales of recruitment limitation in southern Appalachian forests. Ecological Monographs **68**:213–235.

Clark, J. S., and J. S. McLachlan. 2003. Stability of forest biodiversity. Nature **423**:635–638.

Clark, J. S., M. Silman, R. Kern, E. Macklin, and J. Hille Ris Lambers. 1999*b*. Seed dispersal near and far: generalized patterns across temperate and tropical forests. Ecology **80**:1475–1494.

Comins, H. N., and I. R. Noble. 1985. Dispersal, variability, and transient niches: species coexistence in a uniformly variable environment. American Naturalist **126**:706–723.

Connell, J. H., and R. O. Slatyer. 1977. Mechanisms of succession in natural communities and their role in community stability and organization. American Naturalist **111**:1119–1144.

Downs, A. A., and W. E. McQuilkin. 1944. Seed production of southern Appalachian oaks. Journal of Forestry **42**:913–920.

Gelfand, A. E., and D. K. Dey. 1994. Bayesian model choice: asymptotics and exact calculations. Journal of the Royal Statistical Society B **56**:501–514.

Gelfand, A. E., and A. F. M. Smith. 1990. Sampling-based approaches to calculating marginal densities. Journal of the American Statistical Association **85**:398–409.

Gelman, A., J. B. Carlin, H. S. Stern, and D. B. Rubin. 1995. Bayesian data analysis. Chapman and Hall, London, UK.

Gelman, A., and D. B. Rubin. 1992. Inference from iterative simulation using multiple sequences. Statistical Science **7**: 457–511.

Greenberg, C. H., and B. R. Parresol. 2002. Dynamics of acorn production by five species of southern Appalachian oaks. Pages 149–172 *in* W. J. McSchea and W. M. Healy, editors. Oak forest ecosystems. Johns Hopkins University Press, Baltimore, Maryland, USA.

Harper, J. L. 1977. Population biology of plants. Academic Press, New York, New York, USA.

Hastings, A. 1980. Disturbance, coexistence, history, and competition for space. Theoretical Population Biology **18**: 363–373.

Hastings, W. 1970. Monte Carlo sampling methods using Markov chains and their applications. Biometrika **57**:97–109.

Herrera, C. M., P. Jordano, J. Guitián, and A. Traveset. 1998. Annual variability in seed production by woody plants and the masting concept: reassessment of principles and relationship to pollination and seed dispersal. American Naturalist **152**:576–594.

Hixon, M. A., S. W. Pacala, and S. A. Sandin. 2002. Population regulation: historical context and centemporary challenges of open vs. closed systems. Ecology **83**:1490–1508.

Holmes, E., and H. Wilson. 1998. Running from trouble: long-distance dispersal and the competitive coexistence of inferior species. American Naturalist **151**:578–586.

Horn, H. S., and R. H. MacArthur. 1972. Competition among fugitive species in a harlequin environment. Ecology **53**: 749–752.

Hubbell, S. P. 2001. The unified neutral theory of biodiversity and biogeography. Princeton University Press, Princeton, New Jersey, USA.

Huston, M., and T. Smith. 1987. Plant succession: life history and competition. American Naturalist **130**:168–198.

Kelly, D. 1994. The evolutionary ecology of mast seeding. Trends in Ecology and Evolution **9**:465–470.

Kelly, D., and V. L. Sork. 2002. Mast seeding in perrenial plants: Why, how, where? Annual Review of Ecology and Systematics **33**:427–447.

Koenig, W. D., and J. M. H. Knops. 2000. Patterns of annual seed production by northern hemisphere trees: a global perspective. American Naturalist **155**:59–69.

Koenig, W. D., R. L. Mumme, W. J. Carmen, and M. T. Stanback. 1994. Acorn production by oaks in central coastal California: variation within and among years. Ecology **75**:99–109.

LaDeau, S., and J. S. Clark. 2001. Rising CO_2 and the fecundity of forest trees. Science **292**:95–98.

Laird, N. M., and J. H. Ware. 1982. Random-effects models of longitudinal data. Biometrics **38**:963–94.

Lande, R. 1988. Demographic models of the Northern Spotted Owl (*Strix occidentalis caurina*). Oecologia **75**:601–607.

Lange, N., B. P. Carlin, and A. E. Gelfand. 1992. Hierarchical Bayes models for the progression of HIV infection using longitudinal CD4 T-cell numbers. Journal of the American Statistical Association **87**:615–631.

Levine, J. M., and M. Rees. 2002. Coexistence and relative abundance in annual plant assemblages: the roles of competition and colonization. American Naturalist **160**:452–467.

Lindsey, J. K. 1999. Models for repeated measurements. Oxford University Press, Oxford, UK.

Oosting, H. J. 1942. An ecological analysis of the plant communities of Piedmont, North Carolina. American Midland Naturalist **28**:1–126.

Pacala, S. W., C. D. Canham, J. Saponara, J. A. Silander, R. K. Kobe, and E. Ribbens. 1996. Forest models defined by field measurements: estimation, error analysis, and dynamics. Ecological Monographs **66**:1–44.

Pacala, S. W., and M. Rees. 1998. Field experiments that test alternative hypotheses explaining successional diversity. American Naturalist **152**:729–737.

Pastor, J., J. B. Aber, C. A. McClaugherty, and J. M. Melillo. 1984. Aboveground production and N and P recycling along a nitrogen mineralization gradient on Blackhawk Island, Wisconsin. Ecology **65**:256–268.

Rees, M., R. Condit, M. Crawley, S. Pacala, and D. Tilman. 2001. Long-term studies of vegetation dynamics. Science **293**:650–655.

Ribbens, E., J. A. Silander, and S. W. Pacala. 1994. Seedling recruitment in forests: calibrating models to predict patterns of tree seedling dispersion. Ecology **75**:1794–1806.

Sharp, W. M. 1958. Evaluating mast yields in the oaks. Bulletin 635. Agricultural Experiment Station, College of Agriculture, Pennsylvania State University, University Park, Pennsylvania, USA.

Spiegelhalter, D. J., N. G. Best, B. P. Carlin, and A. van der Linde. 2002. Bayesian measures of model complexity and fit (with discussion). Journal of the Royal Statistical Society B **64**:583–639.

Thomas, S. C. 1996. Reproductive allometry in Malaysian rain forest trees: biomechanics versus optimal allocation. Evolutionary Ecology **10**:517–530.

Tilman, D. 1994. Competition and biodiversity in spatially structured habitats. Ecology **75**:2–16.

Warner, R. R., and P. L. Chesson. 1985. Coexistence mediated by recruitment fluctuations: a field guide to the storage effect. American Naturalist **125**:769–787.

Wright, S. J., H. C. Muller-Landan, R. Condit, and S. P. Hubbell. 2003. Gap-dependent recruitment, realized vital rates, and size distributions of tropical trees. Ecology **84**:3174–3185.

APPENDIX

Markov-chain Monte Carlo algorithms, together with prior parameter values, marginal posteriors, a discussion of convergence, and examples using *Acer rubrum* are available in ESA's Electronic Data Archive: *Ecological Archives* M074-010-A1.